# THE STRUCTURE AND HYDRATION OF THE HUMITE MINERALS

by

SARAH MARIE HIRNER

B.S. University of Missouri at Columbia, 2012

A thesis submitted to the

Faculty of the Graduate School of the

University of Colorado in partial fulfillment

of the requirement for the degree of

Master of Science

2013

This thesis entitled:

The structure and hydration of the humite minerals

written by Sarah Marie Hirner

has been approved for the Department of Geological Sciences

Joseph R. Smyth

Steven J. Mojzsis

Alexis S. Templeton

November 22, 2013

The final copy of this thesis has been examined by the signatories, and we find that both the content and the form meet acceptable presentation standards of scholarly work in the above mentioned disciple.

Hirner, Sarah Marie (M.S., Geology, Department of Geological Sciences)

The structure and hydration of the humite minerals

Thesis directed by Professor Joseph R. Smyth

The entire water budget of the mantle may be dominated by nominally anhydrous minerals. The local structural environment of H in the humite minerals could provide a valuable model for the incorporation of H into olivine due to their structural similarities. It also thought that humites may play a significant role in the transport of water into the mantle. Four crystals of chondrodite, clinohumite, norbergite, and humite, both natural and synthetic, have been analyzed via Raman spectroscopy and electron microprobe analysis. Their structures have been refined by single-crystal X-ray diffraction analysis. The new data confirms earlier studies of cation ordering and hydration geometry, and adds new insight into the crystal chemistry of the humite minerals, particularly the geometry of the H position. In humite, hydrogen was found to occupy the H1 site.

## ACKMOWLEDGEMENTS

This research was supported in part by National Science Foundation grants to Joseph R. Smyth.

I would like to thank Dr. Joseph R. Smyth for providing guidance and support through my progress in the study presented in this work. Working with Dr. Smyth has been a wonderful experience, academically and personally. I would also like to thank the faculty and staff in the Department of Geological Sciences at the University of Colorado – Boulder, especially my committee members Alexis Templeton and Steven Mojzsis, who have broadened my academic horizons in the classroom.

I would like to thank several remarkably talented undergraduate students who have assisted me in many experiments, Jacqueline Stonebraker and Steven Chase. Zhenhuan Chi also has my appreciation for his help in obtaining Raman spectra. Finally, I would like to thank my friends and family for their support throughout my graduate career.

**CONTENTS**

**FIGURES**

Figure

## Chapter 1: Introduction

### The humite minerals

Humites are a group of minerals represented by the formula $n Mg_2SiO_4.Mg_{1-x}Ti_x(F,OH)_{2-2x}O_{2x}$ where n = 1 (norbergite), 2 (chondrodite), 3 (humite), or 4 (clinohumite). A simplified formula is also used: $n Mg_2SiO_4 \cdot Mg(F,OH)_2$ (Camara, 1997). The humite structures closely resemble that of olivine, with zigzag chains of edge-sharing $MO_6$ octahedra linked by Si tetrahedral occurring along the *c* axis.

Since the space group of olivine in *Pbnm*, the space groups of the humites are analogously arranged so that the *a*, and *b* axes are retained throughout the humite series. The *a*-axis and *b*-axis in the humites are fixed to 4.7 Å and 10.4 Å approximately. The *c*-axis varies according to the number and pattern of M octahedral that compose the zigzag chains. The primary difference between olivine and the humite minerals is the incorporation of monovalent F or OH anions as ligands. The number per unit volume increases with decreasing *n*. The humites lie on the forsterite-brucite join of the $MgO$-$Mg(OH)_2$-$SiO_2$ system (Smyth, 2006).

The structures of the humites can be described by alternating layers of olivine, $(Mg,Fe)_2SiO_4$, and brucite/sellaite The array of atoms can be described as a distorted hexagonal close-packed anions connected by interstitial cations (Prasad and Sarma, 2004). The distortion of the array has been attributed to cation-cation repulsion across shared edges (Gibbs and Ribbe, 1969). In all the humite minerals, one-half of the octahedral voids are occupied by the cations, while the occupancy of the tetrahedral voids decreases from 1/9 in clinohumite to 1/12 in norbergite (Langer et al., 2002).

Humites always contain Mg, but have also been seen to incorporate $Fe^{2+}$, Mn, Ni, Ca, Cu and Zn (Friedrich et al., 2001). In all humites, all oxygens are coordinated to one Si and 3 *M*-cations, as in olivine (Robinson et al., 1973).

There are three distinct octahedral sites in the humite minerals. *M*(1) shares four edges with octahedra and two with tetrahedra. By convention, *M*(2) share two edges with octahedra and one with tetrahedra. The number of oxygen ligands in an *M*(2) polyhedron is denoted by a subscript. For example, $M(2)_5$ is an octahedral site with two shared octahedal edges and a ligancy of $O_5$(F,OH). *M*3 shares edges with two octahedra and one with an *M*3 octahedron and Si the smallest site in the cell. The two *M*3 sites are related by a center of symmetry and share an edge frequently defined by monovalent anions.

There are three four-coordinated oxygen atoms in all the humite structures, and one (F,OH,O) position. This monovalent anion site in the center of a common structure between all humite minerals, and has been denoted O5. This work will consistently refer to the site as O5 as does Abbot (1989); this is simply a site name and is not indicative of the occupancy of the site. The monovalent anion position is coordinated to two three M sites (Gibbs and Ribbe, 1970). Under Pauling's electrostatic valence principle, O5 site is underbonded. Monovalent anions therefore order to the O5 site in order to stabilize the lack of positive charge this site receives.

*Structure of chondrodite*

Chondrodite has repeating chains of octahedra in groups of five, creating a monoclinic cell that belongs to the space group $P2_1/b$ (Gibbs and Ribbe, 1970). The repeating chains are pictured in Figure 1. The cell parameters for a natural, low iron sample of chondrodite are $a$ = 4.7284(3), $b$ = 10.2539(3), and $c$ = 7.8404(2) Å, $\alpha$ = 109.059(2)° (Gibbs and Ribbe, 1970). Half of the octahedral sites and one-tenth of the tetrahedral sites are filled (Gibbs and Ribbe, 1970). There are three different *M* octahedra, distinguished by their ligancy as represented in Table 1.

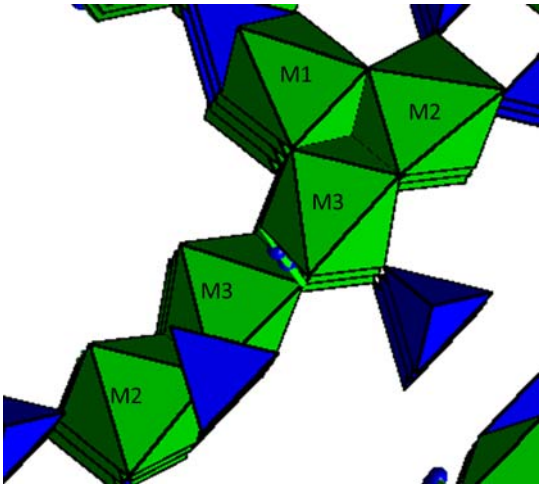


**Figure 1.** Repeating chains of octahedron in chondrodite with interstitial Si tetrahedron. Unit cell is oriented looking down the *a*-axis. (Ottanili et al., 2000)

| **Mineral** | **Octahedral site** | **Edges Shared with Octahedron** | **Edges Shared with Tetrahedron** | **Ligancy** |
|---|---|---|---|---|
| Chondrodite$_{(1)}$ | $M(1)$ | 4 | 2 | $O_6$ |
| | $M(2)_5$ | 2 | 1 | $O_5(F,OH)$ |
| | $M(3)$ | 2-M(1)/M(2)<br>1-M(3) | 1 | $O_4(F,OH)_2$ |
| Clinohumite$_{(2)}$ | $M(1)_c$ | 2-M(1)$_N$<br>2-M(2)$_6$ | 2-Si(1) | $O_6$ |
| | $M(1)_N$ | 1-M(1)$_c$<br>1-M(2)$_5$<br>1-M(2)$_6$<br>1-M(3) | 1-Si(1)<br>1-Si(2) | $O_6$ |
| | $M(2)_6$ | 1-M(1)$_c$<br>1-M(1)$_N$ | 1-Si(1) | $O_6$ |
| | $M(2)_5$ | 1-M(1)$_N$<br>1-M(3) | 1-Si(2) | $O_5(F,OH)$ |
| | $M(3)$ | 1-M(1)$_N$<br>1-M(2)$_5$<br>1-M(3) | 1-Si(2) | $O_4(F,OH)_2$ |
| Norbergite$_{(3)}$ | $M(2)$ | 2 | 1 | $O_4F_2$ |
| | $M(3)$ | 2-M(3)<br>1-M(2) | 1 | $O_4(F,OH)_2$ |
| Humite$_{(4)}$ | $M(1)$ | 4 | 2 | $O_6$ |
| | $M(2)_6$ | 2 | 1 | $O_6$ |
| | $M(2)_5$ | 2 | 1 | $O_5(F,OH)$ |
| | $M(3)O_4(F,OH)_2$ | 2-M(1)/M(2)<br>1-M(3) | 1 | $O_4(F,OH)_2$ |

**Table 1.** Description of the octahedral sites of the humites and corresponding ligancies. References: (1) Gibbs and Ribbe, 1970 (2) Robinson et al., 1973 (3) Gibbs and Ribbe, 1969 (4) Ribbe and Gibbs, 1971.

*Structure of clinohumite*

Clinohumites are thought to be the humite mineral most closely related to olivine. In olivines 1/8 of the tetrahedral sites are filled and clinohumites have the highest occupancy of tetrahedral sites among the humites (Robinson et al., 1973). Unit cell parameters for a non-Ti-bearing, natural sample of clinohumite are *a*=4.7441(2), *b*=10.2501(5), *c*=13.6635(3) Å, α~~lpha~~=100.876(2)° (Robinson et al., 1973). Clinohumite also falls within the $P2_1/b$ space group. Unlike chondrodite, clinohumite has five unique *M* octahedra.

The chains in clinohumite can be divided into four segments and described as follows: (1) $M2_5$-M3-M3-$M2_5$, (2) $M2_5$-$M1_N$-$M2_6$, (3) $M2_6$-$M1_c$-$M2_6$, and (4) $M2_5$-$M1_N$-$M2_5$ (Robinson et al., 1973).

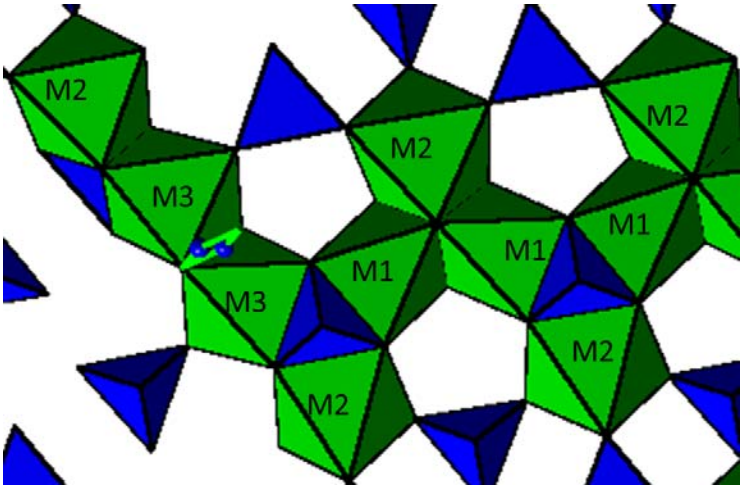


**Figure 2.** Repeating chains of octahedron in clinohumite with interstitial Si tetrahedron. Unit cell is oriented looking down the *a*-axis. (Ottanili et al., 2000)

*Structure of norbergite*

Norbergite has repeating chains of octahedra in groups of six, creating an orthorhombic cell with a space group of *Pbnm*. like olivine. The cell parameters of a natural, pure Mg norbergite are *a* = 4.7104(1), *b* = 10.2718(3), *c* = 8.7476(4) Å (Gibbs and Ribbe, 1969).

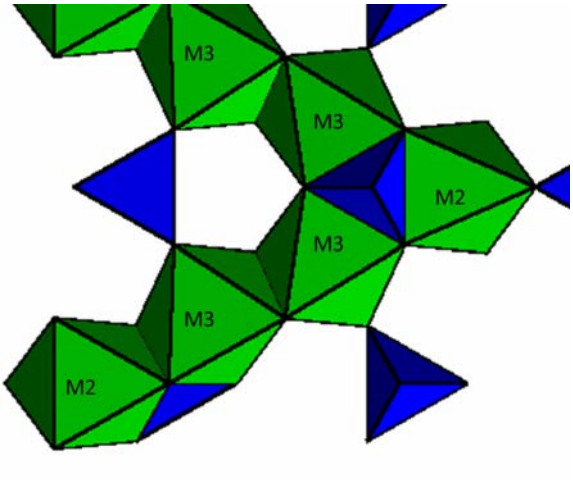


**Figure 3.** Repeating chains of octahedron in norbergite with interstitial Si tetrahedron. Unit cell is oriented looking down the *a*-axis. (Gibbs and Ribbe, 1969)

Norbergite is the only mineral that exhibits two of the three distinct cation sites. The *M*2 site has ~~$C_s$~~ point symmetry *m* and ligancy of $O_4F_2$. In addition, the *M*(3) is distinct from the M3 site in all other humites, sharing edges with two M3 sites. One of these edges is an F-F edge, the other is an O-O edge.

*Structure of humite*

Humite shares the same space group as norbergite and olivine. The cell parameters of a natural, low iron sample of humite are *a* = 4.7408(1), *b* = 10.2580(2), *c* = 20.8526(4) Å (Ribbe and Gibbs, 1971).

Humite's repeating chain structure can be divided into three segments: (1) M2-M1-M2, (2) M2-M3-M3-M2, and (3) M2-M1-M2.

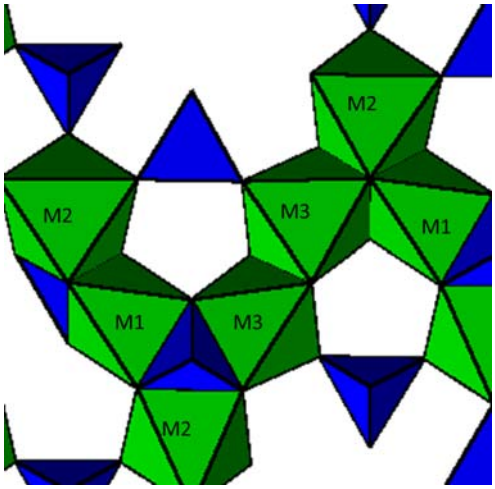


**Figure 4.** Repeating chains of octahedron in humite with interstitial Si tetrahedron. Unit cell is oriented looking down the *a*-axis. (Ribbe and Gibbs, 1971).

A pure hydroxyl calcium analogue of humite called chegemite has been recently discovered in xenoliths in the Upper Chegem volcanic structure in Russia (Galuskin et al., 2009).

**Hydrogen in the mantle**

Liquid water covers 70% of the Earth, driving all of its surface processes. However, this water is only 0.025% of the Earth's mass. Carbonaceous chondrites have up to 0.1 wt % water, leaving scientists with the question: Where did Earth's water go? Measured water contents of natural basalts, such as melt inclusions trapped in olivine, suggest water could be trapped in the Earth's interior (Bolfan-Cassanova, 2000). Hydrated xenoliths have suggested that the storage capacity of water is greater at depth. These studies have presented the idea that there may be significant amounts of water as H defects in oxygen minerals in the Earth. If water is being recycled through deep Earth processes, it is possible that the oceans move through the mantle every 100 to 1000 million years.

Empirical studies have revealed that water in the mantle is most likely carried into the mantle by dense hydrous mineral phases such as chondrodite, and stored in nominally anhydrous minerals (NAMs) such as olivine, pyroxene, garnet, and their high-pressure polymorphs. Water is incorporated to

minerals as hydroxyl point defects, and becomes more soluble at with increasing depth (Bolfan-Cassanova, 2000). Hydrogen usually occurs as M-O-H bonds rather than silanyl groups. The silanyl group bonds are shorter, causing more strain than the M-O-H structure.

The local structural environment of H in the humite minerals could provide a valuable model for the incorporation of H into olivine due to their structural similarities. It is thought that the entire water budget of the mantle may be dominated by nominally anhydrous minerals (Bell and Rossman, 1982). It also thought that humites may play a significant role in the transport of water into the mantle. Understanding the process of hydrogen incorporation in humite minerals will therefore enable a deeper understanding of the mineralogical role of the Earth's water cycle.

**Hydrogen in the humites**

Humite minerals are nominally hydrous minerals and incorporate H as a point defect associated with the monovalent anion site in each mineral. Water is incorporated into the humite structures as a hydrated, Si-deficient layer (Berry and James, 2002) as depicted in Figure 5. This layer can be described as Mg(F,OH)O, where Mg corresponds to the M3 site (Berry and James 2002).

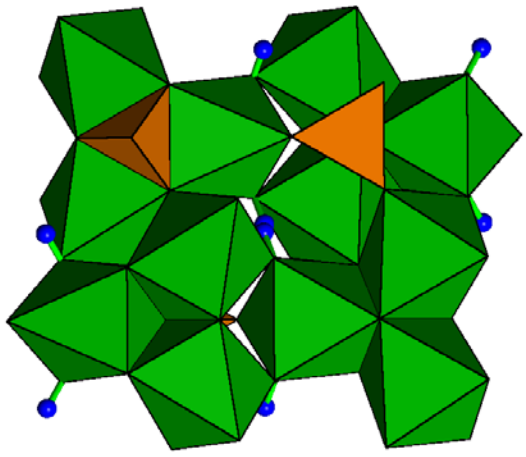

**Figure 5**. Si-deficient hydrogen layer in a natural, pure Mg norbergite. Hydrogen atoms are depicted as blue spheres. Si-tetrahedron are depicted with orange polygons.

OH-end-members, or fully hydroxylated humites, are rarely found in nature. Only one natural end-member has been identified. This was OH-clinohumite and was found as megacrysts in ultramafic serpentine veins (Freidrich et al., 2001). However, OH-end-members of the humite group have successfully been synthesized in the laboratory (Yamamoto and Akimoto, 1977; Akaogi and Akimoto, 1986, Wunder, 1995). OH-chondrodite and OH-clinohumite have been successfully synthesized multiple times; however, synthesis of OH-humite has only been reported once. OH-norbergite has never been synthesized.

The humites have been found to occupy two distinct hydrogen sites via X-ray diffraction studies (Yamamoto and Akimoto, 1977) and structure-energy calculations (Abbott et al., 1989). H1 and H2 are both associated with the O5 site.

Hydrogen occurs in the structure as a centrosymmetric pair at H1. This centrosymmetric pair occurs along an edge defined by two monovalent anions and within a cavity surrounded by two M(2) octahedra, four M(3) octahedra, and two Si(2) terahedra as depicted in Figure 6. The M(3) sites that define this cavity are also related by the center of symmetry (Berry and James,2002).

H2 is located in a cavity composed of two *M*(2) octahedra, two *M*(3) octahedra, one *M*(1) octahedra, and one Si(2) octahedra (Berry and James, 2002).

Whether H1 or H2 is the primary site of H incorporation in the humite minerals has long been a topic of debate. Structure-energy calculations have identified H2 as the primary site under identical substitution conditions (Abbott et al., 2002). However, x-ray diffraction and neutron diffraction studies have consistently found H1 to be the occupied site under various substitution conditions (Camara, 1997, Fujino and Takeuchi, 1978, Friedrich et al., 2001 and 2002). Neutron diffraction studies have revealed that H2 experiences minimal hydrogen bonding relative to H1, and provided support for H1 as the primary hydrogen position (Berry and James, 2001).

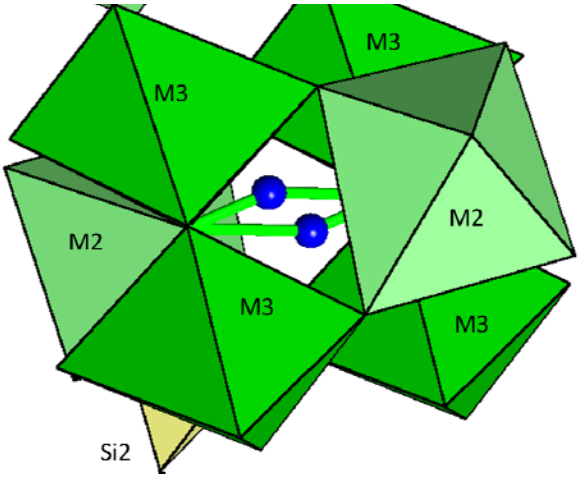


**Figure 6.** H1 position in a natural low-iron sample of chondrodite. (Ottolini et al., 2000).

The H1 and H2 sites can be distinguished by the orientation of their OH vectors. This orientation is described by the angle between the *a*-axis and the OH vector (Abbott et al., 1989). Calculated H2 sites have been reported to have *a*-O5-H2 angles between 25 and 60°. Calculated H1 sites have a-O5-H1 angle between -80 and -140°. These vectors ~~are~~ oppose each other in orientation and when both sites are hydroxylated, this provides some counteraction to the hydrogen-hydrogen repulsion (Berry and James, 2002).

The sites can also be described by their hydrogen bonding relationships to neighboring anions. The H1 position forms one nearly linear and one nearly bent hydrogen bond, whereas H2 forms two bent hydrogen bonds. Because of the angles and lengths of the hydrogen bonds associated with the H2 site, the H2 H-bonds are thought to stabilize the structure much less than the H1 H-bonds (Berry and James, 2001).

Due to space group constraints, two H sites are approximately 1 Å from each other. The H-H interaction destabilizes the structure and places a constraint on hydrogen occupancy pertaining to this site. If hydrogen occupancy is limited to the H1 site, only 1hydrogen per formula unit is possible.

Yamamoto and Akimoto (1977) proposed a parity rule stating that neighboring hydrogens occupy different kinds of sites. That is, when full hydroxylation occurs, the nearest neighbor to an occupied H1 site will occupy an H2 site. This has been confirmed by structure energy calculations. The occupancy of both the H1 and H2 site enables OH-rich humites to occur and avoids the destabilizing H ··· H interactions associated with full occupancy of the H1 site (Berry and James, 2001).

Several significant substitutions, including $F^-$ and $Ti^{4+}$ effect hydrogen incorporation in the humite minerals. It has previously been thought that the substitution of F into the O5 monovalent anion site stabilized the structure by minimizing hydrogen repulsions. However, it has been shown that fully hydroxylated end-members are made possible by the opposing O-H vectors generated by the two H positions.

*Hydrogen in norbergite and humite.*

Pure OH-norbergite has never been synthesized, and OH-rich samples are rare, which could be attributed to the known sample size (Camara, 1997). An OH-rich natural sample has been found, with the H position correlated to the H1 position identified by Yamamoto and Akimoto (1977).

OH-humite was synthesized by Wunder et al. (1995). However, the hydrogen position was not refined, and structural information about the interaction of hydrogen and humite is so far lacking. This work will present the first location of hydrogen atoms in the humite structure via X-ray diffraction analysis.

*Hydrogen bonding*

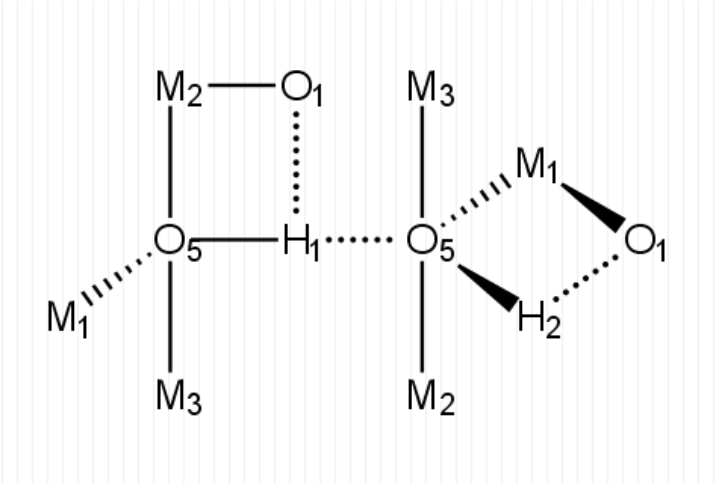


**Figure 7.** Local hydrogen bonding environment in the humites.

The O5 atom is both a donor and acceptor in hydrogen bonding. There is one strong and one weak H bond associated with the H1 site in both the clinohumites and F-bearing chondrodite. The strong bond can be characterized by O5-O5 bond distances and the weak bond can be characterized by O5-O1/O2,2 bond distances (Friedrich et al., 2002). The O5-O5 bond is lengthened with increasing protonation; whereas the O5-O2,2/O1 decreases is length due to H-bonding, and increases in the absence of H due to anion-anion repulsion.

Hydrogen bonding plays a significant role in the determination of the structure of the humite minerals. The F/(F+OH)ratio in natural humite minerals is nearly always approximately 0.5 (Berry and James, 2002). Hydrogen bonding is maximized at this ratio, and therefore this ratio remains relatively constant across humite minerals formed in different chemical environments$Ti^{4+}$ substitution is also partly governed by hydrogen bonding. An upper limit of an occupancy of 0.25 is imposed $Ti^{4+}$. At occupancies up to 0.25, every O5 with a charge imbalance can be stabilized by a H bond.

**Cation Ordering in the humites**

*Iron*

The first cation ordering observed in the humites was observed with $Fe^{2+}$ (Gibbs and Ribbe, 1969). $Fe^{2+}$ has been observed to occupy sites with no monovalent anion positions (Ribbe and Gibbs, 1971). In chondrodite, this is the M1 site. In clinohumite, $Fe^{2+}$ substitutes in a relatively equal amounts between M1 and $M2_6$ (70 to 90% of the $Fe^{2+}$ in these samples order to these sites). Analogously to clinohumite, Fe ordering would be expected to occur in the M1 and $M2_6$ site in humite.

$Fe^{2+}$ selects sites that are not only free of F,OH ligands, but also the largest, most distorted polyhedra in each mineral. It seems that the ordering of $Fe^{2+}$ is dictated by the distortion of the site and the polarizability of the ligands (Ribbe and Gibbs, 1971).

*Titanium*

$Ti^{4+}$ substitution is governed by charge imbalances. In fact, prior to extensive hydrogen bonding investigations, the patterns of Ti substation were thought to be controlled primarily by Pauling's electrostatic valence principle (Ribbe, 1979). $Ti^{4+}$ becomes incorporated into sites with the most underbonded monovalent anion positions, and is accompanied by increased oxygen in these sites according the following mechanism.

$$Mg + 2(OH,F) \rightarrow Ti + 2(O) + \square$$

The site with the most monovalent anion positions is the M3 site. These sites remain underbonded, but by a reduced amount, and are therefore optimum positions for protons. If $Ti^{4+}$ were to occupy the M3 site with more than 0.25 occupancy, the structure would be destabilized by the charge imbalance. Additional evidence for $Ti^{4+}$ ordering was provided by Fujino, who found that intergrown

specimens of Ti-chondrodite and Ti-clinohumite had Ti/Si rations twice as high in Ti-chondrodite as in Ti-clinohumite. The M3/Si ratio is 2 in chondrodite and 1 in clinohumite.

The presence of highly charged cations such as $Ti^{4+}$ and possibly $Fe^{3+}$ demands divalent cations, and therefore there is a negative correlation between $F^-$ and $Ti^{4+}$ in the humite minerals (Robinson et al., 1973). It has been suggested that F is incorporated preferentially over Ti, and therefore the amount of F in a mineral controls the level of $Ti^{4+}$ that can enter the structure (Ribbe, 1979). The only OH-end member found in nature was Ti-bearing, suggesting that the presence of Ti enables protonation of the humite structure.

In nature, clinohumite is commonly Ti-rich, whereas chondrodite and norbergite seem to lack significant Ti-incorporation in nature. The occurrences of Ti-rich clinohumite and chondrodite are limited to a kimberlite inclusion sample, whereas Ti-free samples are found in multiple natural samples of metamorphosed dolomites and limestones (Fujino and Takeuchi, 1978). Because of the higher M3/Si ratio of chondrodite, the maximum weight percent $TiO_2$ chondrodite can incorporate is approximately 10.19 weight percent, whereas clinohumite's maximum Ti-load is approximately 5.7 weight percent (Fujino and Takeuchi, 1978).

## Chapter 2: Methods

### Samples and Synthesis

This study analyzed four humite samples. The chondrodite sample came from a synthetic experiment S0407B and was a pale yellow and translucent. The starting materials were brucite and San Carlos olivine, a natural Fe-bearing (Fo90) olivine. Synthesis conditions were 12.0 GPa and 1250 °C, and a polyphase sample was formed with a gradient of minerals including phase A, chondrodite, clinohumite, and olivine.

The norbergite sample was a natural sample from Franklin, New Jersey. It was a transparent, pale orange crystal taken found in a hand sample with calcite.

The humite sample was a natural sample from the Tilly Forster mine in Brewster, New York. It was a transparent, dark orange-brown crystal. The Tilly Foster mine is a magnetite deposit that occurs in a marble (Buddington, 1966).

The clinohumite sample was from Danbury, Connecticut, and was part of a bulk, fragmented mineral sample. The crystals appeared pale yellow and translucent.

### X-ray diffraction

The humite samples were analyzed with a single-crystal 4-circle diffractometer with a dual scintillation point detector system at the University of Colorado. The generate voltage was 50 kV and the current 250 mA for all experiments. The unit-cell parameters were refined by a least-squares refinement of the data from the point detector. Both detectors are mounted on Bruker P4 four-circle diffractometers on an 18 kW rotating Mo-anode X-ray generator. Mo radiation was used ($K\alpha_1$ = 0.709300 Å, $K\alpha_2$ = 0.713590 Å). Kα(mix)=0.71093 Å, determined by the percentages of K $\alpha_1$ and $K\alpha_2$. We

used a perfect single crystal of ruby near sphere shape to calibrate the Kα(mix), i.e., the wavelength used for all cell refinement. The 2θ range for all reflections was limited from 12 to 70°. After centering of all reflections, a least-squares fitting was done to calculate the cell parameters with uncertainties.

Intensity data were collected using a Bruker Apex II CCD detector. Refinements of atom positions and anisotropic displacement parameters and ionized scattering factors were completed using the program SHELX-97 (Sheldrick 1997)in the software package WinGC (Farrugia 1999). The chondrodite structure was refined in the space group $P2_1/b$. The norbergite and humite structures were refined in the space group *Pbnm*.

For the humite sample, residual maxima were indicated after convergence of weighted full-matrix least-squares refinements carried out with SHELX-93 (Sheldrick 1993). The highest maximum had a peak height of 0.64 $e/Å^3$ and was set at 0.79 Å from O5. The second highest maximum had a peak height of 0.61 $e/Å^3$ and was 0.59 Å from O5. The highest peak was inserted into the structure and refined first, and this was repeated with second position. Each of the maxima were inserted as H in the model, and refined without any constraints (*i.e.* occupancy, thermal displacement parameter and fractional coordinates were allowed to vary). The $wR^2$ factor improved significantly.

**Table 2**. Data collection parameters for humite samples in this study.

| | **Chondrodite** | **Clinohumite** | **Norbergite** | **Humite** |
|---|---|---|---|---|
| **No. unique Total** | 1913 | 1899 | 767 | 1191 |
| **No. unique *I*>4σ** | 1831 | 2538 | 624 | 878 |
| **GooF** | 1.623 | 1.226 | 2.899 | 1.142 |
| **$R_1$ for *I*>4σ (%)** | 2.13 | 4.54 | 4.73 | 3.76 |
| **$R_{int}$(%)** | 2.23 | 5.48 | 7.32 | 5.72 |

**Raman Spectroscopy**

Raman spectra at room temperature and pressure were collected with a Renishaw inVia reflex Raman microscope spectrometer system, and the spectra were obtained with the 532 and 785 nm line from an argon ion laser. The spectra were recorded with a 50X Leica DM2500 microscope objective with

integration times ranging from 1 – 10 s with 30 mW power on the sample. The focused laser spot was estimated to be approximately 2 - 4 μm in diameter.

**Electron Microprobe Analysis**

The four samples were mounted in epoxy and polished. They were analyzed for Si, Mg, $Fe^{2+}$, Mn, Ti, Al, Cr, Na, and F with a JOEL JXA-8600 Superprobe at the University of Colorado. Forumulas for chondrodite were calculated by normalizing the chemical analysis to 10 oxygen atoms and the following general formula $M_5Si_2O_8(F,OH)_2$. For clinohumite, the chemical analysis was normalized to 18 oxygen atoms and the following formula: $M_9(SiO_4)_4(F,OH)_2$. For norbergite, the chemical analysis was normalized to six oxygen atoms and the following formula: $M_3SiO_4(F,OH)_2$. Humite was normalized to 14 oxygen atoms the following formula: $M_7(SiO_4)_3(F,OH)_2$.

## Chapter 8: Results

Electron microprobe analysis revealed that the natural norbergite sample exhibited very low Fe contents compared to the chondrodite, clinohumite, and humite samples, shown in Table 3. Since $Fe^{2+}$ orders to distortable sites with no monovalent anions, and norbergite has no such sites, the lack of incorporation of $Fe^{2+}$ into norbergite confirms the preference of $Fe^{2+}$ to such distortable sites.

The F content in norbergite is high, reinforcing the literature description of norbergite as an F-dominant species. However, norbergite is a rare mineral in nature, and thus conclusions may be misleading due a small sample size (Camara, 1997). Both the humite and the norbergite sample are relatively OH- and Ti-rich when compared to literature values.

**Table 3.** Compositions of humite samples used in the present study.*The averages of 3-4 analyses in each sample.*Calculated by stoichiometry.

| **Composition (in wt %)** | **Chondrodite** | **Clinohumite** | **Norbergite** | **Humite** |
|---|---|---|---|---|
| **$SiO_2$** | 34.45 | 36.80 | 29.05 | 35.95 |
| **$TiO_2$** | 0.00 | 0.08 | 0.99 | 0.26 |
| **FeO** | 1.85 | 5.19 | 0.40 | 6.88 |
| **MnO** | 0.00 | 0.22 | 0.02 | 0.23 |
| **MgO** | 55.96 | 53.90 | 58.15 | 52.38 |
| **F** | 0.00 | 2.32 | 11.33 | 2.50 |
| **$H_2O$*** | 5.13 | 1.70 | 3.42 | 2.42 |
| **Total** | 97.13 | 99.24 | 98.60 | 99.55 |
| **In atomic proportions Per how many oxygens??** | | | | |
| **Ti** | 0.00 | 0.01 | 0.03 | 0.016 |
| **Fe** | 0.09 | 0.47 | 0.01 | 0.480 |
| **Mg** | 4.88 | 8.61 | 2.96 | 6.493 |
| **Mn** | 0.00 | 0.02 | 0.00 | 0.016 |
| **F** | 0.00 | 0.79 | 1.22 | 0.658 |
| **OH** | 2.00 | 1.21 | 0.78 | 1.342 |

The following formulas were obtained: OH-chondrodite: $Mg_{4.\ 88}Fe_{0.09}Si_2O_8(OH)_2$, natural clinohumite: $Mg_{8.61}Fe_{0.47}Ti_{0.01}Mn_{0.02}(SiO_4)_4F_{0.79}(OH)_{1.21}$, natural norbergite: $Mg_{2.96}Fe_{0.01}Ti_{0.03}SiO_4F_{1.22}(OH)_{-0.78,}$ natural humite: $Mg_{6.49}Fe_{0.48}Ti_{0.02}Mn_{0.01}(SiO_4)_3F_{0.66}(OH)_{1.34.}$

**Humite**

The unit cell parameters were refined to be a = 4.750(3), b = 10.279(3), c = 20.884(9) Å, and V = 1019.58(68) $Å^3$.

**Table 4.** Atomic fractional coordinates and thermal displacement parameters for natural humite sample from Brewster, NY.

| Atom | *x/a* | *y/b* | *z/c* | occ* | $U_{11}$ | $U_{22}$ | $U_{33}$ | $U_{23}$ | $U_{13}$ | $U_{12}$ | Ueq |
|---|---|---|---|---|---|---|---|---|---|---|---|
| **Si1** | 0.0736(3) | 0.9695(2) | 0.25 | 0.5 | 0.0074(7) | 0.0097(8) | 0.0072(6) | 0.0000(0) | 0.000(0) | 0.0000(6) | 0.0081(4) |
| **Si2** | 0.5760(2) | 0.2816(1) | 0.1059(1) | 1.0 | 0.0070(5) | 0.0085(6) | 0.0076(5) | 0.0001(4) | 0.0002(4) | 0.0000(4) | 0.0077(3) |
| **Mg1** | 0.0017(2) | 0.3771(1) | 0.1767(3) | 0.8627(6) | 0.0068(6) | 0.0095(5) | 0.0065(4) | 0.0013(4) | 0.0011(4) | 0.0006(4) | 0.0076(4) |
| **Fe1** | 0.0017(2) | 0.3771(1) | 0.1767(1) | 0.1372(3) | 0.0068(6) | 0.0095(6) | 0.0065(5) | 0.0013(4) | 0.0011(4) | 0.0006(4) | 0.0076(4) |
| **Mg2** | 0.5119(3) | 0.1543(1) | 0.25 | 0.423(3) | 0.0084(9) | 0.0087(9) | 0.0069(7) | 0.0000(0) | 0.0000(0) | 0.0010(6) | 0.0080(5) |
| **Fe2** | 0.5119(3) | 0.1543(1) | 0.25 | 0.076(3) | 0.0084(9) | 0.0087(9) | 0.0069(8) | 0.0000(0) | 0.0000(0) | 0.0010(6) | 0.0080(5) |
| **$Mg2_5$** | 0.0095(2) | 0.0976(1) | 0.1093(1) | 0.9708(5) | 0.0075(7) | 0.0064(7) | 0.0079(6) | 0.0006(5) | 0.0001(5) | 0.0000(5) | 0.0073(3) |
| **$Fe2_5$** | 0.0095(2) | 0.0976(1) | 0.1093(1) | 0.0291(5) | 0.0075(7) | 0.0064(7) | 0.0079(6) | 0.0006(5) | 0.0001(5) | 0.00000(5) | 0.0073(4) |
| **Mg3** | 0.4927(3) | 0.8669(1) | 0.0277(1) | 0.994(5) | 0.0061(7) | 0.0084(7) | 0.0057(6) | 0.0002(5) | 0.0011(5) | 0.0007(5) | 0.0067(4) |
| **O2,3** | 0.7230(5) | 0.2143(3) | 0.1687(1) | 1.0 | 0.008(1) | 0.009(2) | 0.008(1) | 0.002(1) | 0.000(1) | 0.000(1) | 0.009(6) |
| **O1,3** | 0.2211(5) | 0.0378(3) | 0.1882(1) | 1.0 | 0.008(1) | 0.012(2) | 0.010(1) | 0.000(1) | 0.000(9) | 0.000(1) | 0.0104(7) |
| **O2,4** | 0.7275(5) | 0.2091(3) | 0.0451(1) | 1.0 | 0.007(1) | 0.012(2) | 0.007(1) | 0.002(1) | 0.000(1) | 0.001(1) | 0.0089(7) |
| **O2,1** | 0.2359(5) | 0.2815(3) | 0.1046(1) | 1.0 | 0.008(1) | 0.012(2) | 0.007(1) | 0.002(2) | 0.000(10) | 0.00(10) | 0.0093(6) |
| **O1,2** | 0.2794(7) | 0.3239(4) | 0.2500(0) | 0.5 | 0.010(2) | 0.010(2) | 0.010(2) | 0.0000(0) | 0.0000(0) | 0.002(1) | 0.01(10) |
| **O1,1** | 0.7345(7) | 0.9686(4) | 0.2500(0) | 0.5 | 0.007(2) | 0.007(2) | 0.009(2) | 0.0000(0) | 0.0000(0) | 0.002(1) | 0.0080(9) |
| **O2,2** | 0.2200(5) | 0.9275(3) | 0.1044(2) | 1.0 | 0.008(1) | 0.010(2) | 0.008(1) | 0.000(1) | 0.000(1) | 0.000(1) | 0.0095(6) |
| **O5** | 0.2646(9) | 0.0324(4) | 0.0363(2) | 1.0 | 0.008(1) | 0.015(2) | 0.009(2) | 0.001(2) | 0.000(2) | 0.001(1) | 0.0095(8) |
| **H1** | 0.2004(3) | 0.0227(1) | 0.474(3) | 0.99(1) | 0.00(2) | | | | | | |
| **H2** | 0.3301(4) | 0.0767(1) | 0.027(5) | 0.04(1) | 0.00(9) | | | | | | |

Significant ordering of $Fe^{2+}$ was observed in the crystal refinement of humite. The M1 site exhibits 13.7% $Fe^{2+}$ occupancy and the $M2_6$ site had 7.6% $Fe^{2+}$ occupancy. The M3 site is nearly devoid of iron, with 99.4% $Mg^{2+}$ occupancy. Single-crystal refinements of humite revealed 6.8 mol % occupancy of $Fe^{2+}$, which corresponds to 6.8% determined by microprobe analysis.

Two H positions were identified in the humite sample by X-ray diffraction, shown in Table 4. The H1 site showed significantly higher occupancy and also was a significantly larger peak in the Fourier analysis, and is therefore considered the dominant site. The Raman spectrum of the OH-stretching modes confirms that two different H positions are occupied, shown in Figure 8.

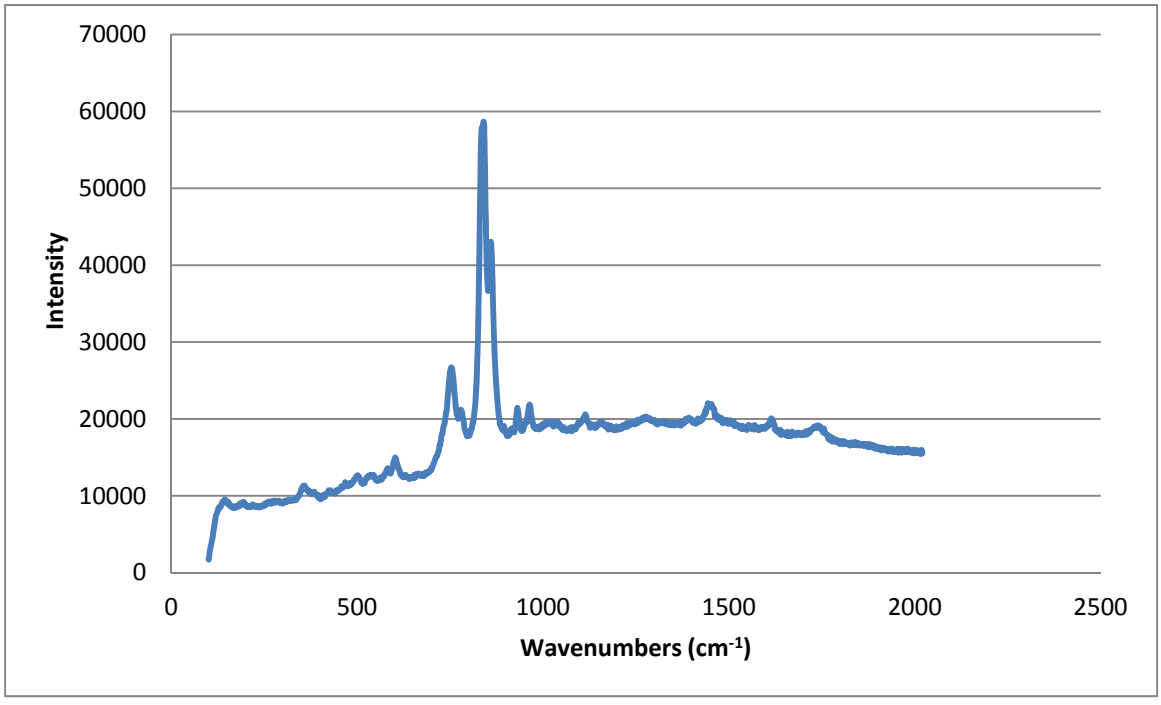


**Figure 8.** Raman spectrum of humite corresponding to the normal vibrational modes at ambient temperature and pressure. Collected with a 532 nm wavelength laser line**.**

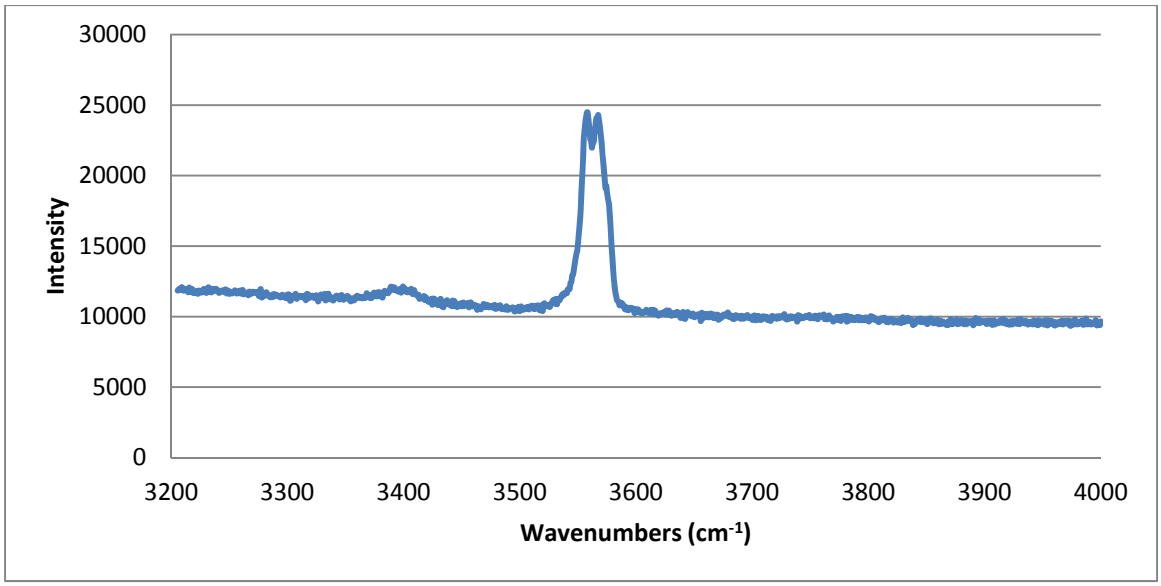


**Figure 9.** Raman spectrum of humite corresponding to the OH-stretching modes at ambient temperature and pressure. Collected with a 532 nm wavelength laser line**.**

The Raman spectrum of the humite sample exhibit a strong-doublet corresponding to the O-H stretching modes of the 2 H positions in the mineral. Four O-H stretching modes are predicted for all the humite samples, two from the O-H1 bond and two from the O-H2 bond. The two strong peaks are observed at 3567 $cm^{-1}$ and 3568 $cm^{-1}$ and have previously been observed by Frost et al. (2006) in a similar natural, Tilly Foster mine humite sample.

One H atom in the humite sample points toward the center of symmetry at the center of a cavity surround by two M(2) octahedra, four M(3) octahedra, and two Si(2) terahedra as shown in Figure 10. This position corresponds to the H1 position as described by Fujino and Takeuchi (1978). Another proton was identified in a cavity defined by *M*(2) octahedra, two *M*(3) octahedra, one *M*(1) octahedra, and one Si(2) octahedra (Berry and James, 2002).

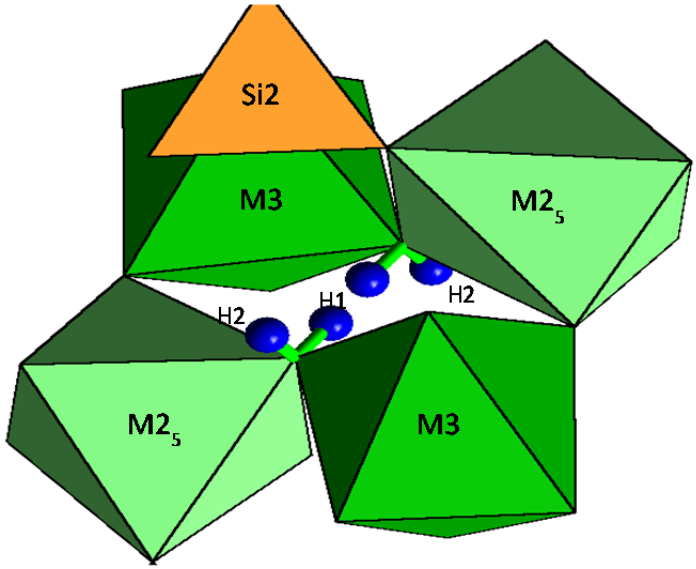


**Figure 10.** H1 and H2 in natural humite sample from Brewster, NY.

The local configuration prevents H occupancy in humite to be higher than 1 atom per formula unit. O-H bonds would need to bend in order to incorporate two hydrogen atoms into the cavity; however, the cation arrangement surrounding the cavity prevents this.

Our site refinement reveals that the H1 and H2 sites match those previously identified in OH-rich chondrodite and clinohumite. This suggests that equivalent H-bonds exist in humite as previously observed.

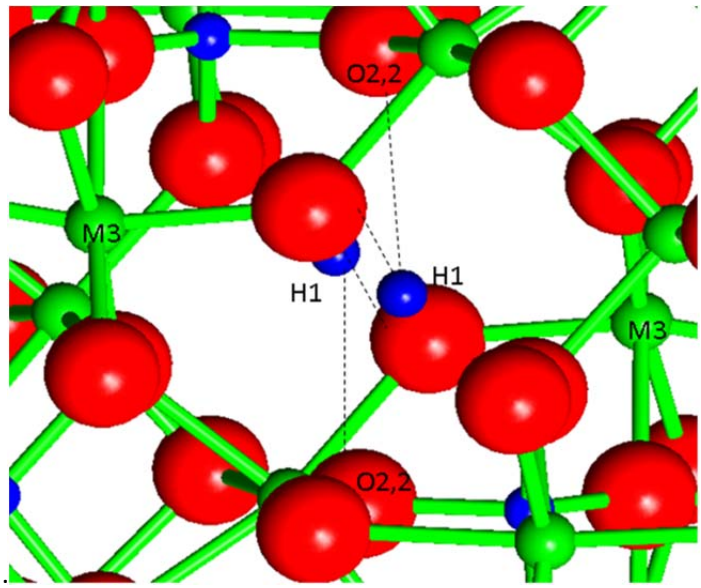


**Figure 11.** H bonding environment in humite (this study).

**Table 5.** Selected interatomic distances (Å) and geometric parameters for natural humite sample from Brewster, NY.

| | | | | | |
|---|---|---|---|---|---|
| **Si1-O1,1** | 1.6305(35) | **$M2_5$-O1,3** | 2.0166(28) | **M3-O2,1** | 2.1200(29) |
| **Si1-O1,2** | 1.6443(43) | **$M2_5$-O2,1** | 2.1672(30) | **M3-O2,2** | 2.1848(30) |
| **Si1-O1,3** | 1.6213(30) | **$M2_5$-O2,2** | 2.0544(28) | **M3-O2,4** | 1.9993(29) |
| **Si1-O1,4** | 1.6443(43) | **$M2_5$-O2,3** | 2.1869(29) | **M3-O2,4** | 2.1191(28) |
| **<Si1-O>** | 1.6226 | **$M2_5$-O2,4** | 2.2058(30) | **M3-O5** | 2.0157(30) |
| **Vol (Å$^3$)** | 2.1585 | **$M2_5$-O5** | 2.0525(40) | **M3-O5** | 2.0392(45) |
| **TQE** | 1.0105 | **<$M2_5$-O>** | 2.0993 | **<M3-O>** | 2.0786 |
| **TAV** | 46.6270 | **Vol (Å$^3$)** | 11.9716 | **Vol (Å$^3$)** | 11.6701 |
| | | **OQE** | 1.0209 | **OQE** | 1.0181 |
| | | **OAV** | 73.4239 | **OAV** | 59.9709 |
| | | | | | |
| **Si2-O2,1** | 1.6083(26) | **$M2_6$-O1,1** | 2.1728(43) | **O5-O5** | 2.7720 |
| **Si2-O2,2** | 1.6315(28) | **$M2_6$-O1,2** | 2.0547(40) | **O5-O2,2** | 2.962 |
| **Si2-O2,3** | 1.6323(31) | **$M2_6$-O1,3** | 2.2280(31) | **O5-H1** | 0.8200 |
| **Si2-O2,4** | 1.6418(29) | **$M2_6$-O1,3** | 2.2280(31) | **O5-H2** | 0.5790 |
| **<Si2-O>** | 1.6450 | **$M2_6$-O2,3** | 2.0854(29) | | |
| **Vol (Å$^3$)** | 2.2297 | **$M2_6$-O2,3** | 2.0854(29) | | |
| **TQE** | 1.0167 | **<$M2_6$-O>** | 2.1334 | | |
| **TAV** | 73.6244 | **Vol (Å$^3$)** | 12.4254 | | |
| | | **OQE** | 1.0291 | | |
| | | **OAV** | 99.5820 | | |

Through careful examination of bond distances and bond angles, it is clear that cation repulsion across shared edges dictates the distortion of the hexagonal close-packed array. This repulsion thus

contributes most significantly to the overall lattice strain. Bond angle strain is defined as the difference between the ideal bond angle (in the case of the humites, corresponding to a hexagonal close-packed array) and the observed bond angle. Results for bond strains of humite of various chemical compositions are depicted in Table 6.

**Table 6.** Selected bond angles indicative of cation-cation repulsion in humite samples of various chemical compositions. References: (1) Gibbs and Ribbe, 1969 (2) This study.

| **Angle** | **0.47 OH/(OH+F)$_{(1)}$** | **0.67 OH/(OH+F)$_{(2)}$** |
|---|---|---|
| **O(1,3)-M1-O(1,2)** | -15.6 | -15.64 |
| **O(1,3)-M2$_6$-O(1,3)** | -19.4 | -19.52 |
| **O(2,4)-M2$_5$-O(2,1)** | -10.0 | -10.23 |
| **O(2,2)-M3-O(2,1)** | -1.9 | -6.69 |

Bond angle strains are directly proportional to the Oh-content of a humite mineral. This trend is most notable in the O(2,2)-M3-O(2,1) angle strain. It is interesting to note that neither the O(2,2) nor O(2,1) site is directly involved in the incorporation of hydrogen. Thus, one may infer that these strains are reflecting the shift of the M3 cation in response to repulsion introduced by the H.

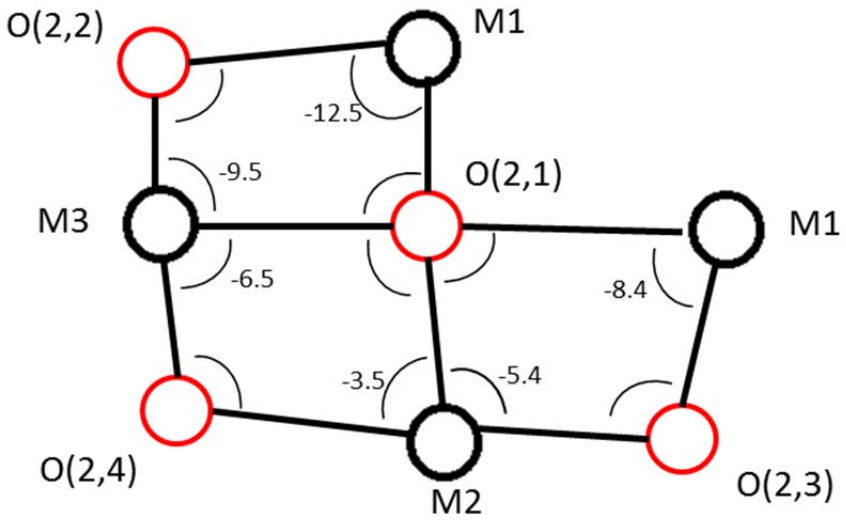


**Figure 12.** The face of a cube in the hexagonal close-packed array in the humite sample. Negative bond angle strains induced by cation repulsion are labeled at the vertices.

**Chondrodite**

The unit cell parameters were refined to be *a* = 4.746(0), *b* = 10.351(1), and *c* = 7.902(1) Å, α = 108.706(7)°, V = 367.74(4) Å$^3$.

**Table 7.** Atomic fractional coordinates and thermal displacement parameters for synthetic chondrodite sample 407B.

| Atom | *x/a* | *y/b* | *z/c* | occ* | $U_{11}$ | $U_{22}$ | $U_{33}$ | $U_{23}$ | $U_{13}$ | $U_{12}$ | Ueq |
|---|---|---|---|---|---|---|---|---|---|---|---|
| **Mg1** | 0.5 | 0.0 | 0.5 | 0.4866(0) | 0.0074(7) | 0.0056(9) | 0.0061(9) | 0.0009(8) | 0.0011(5) | 0.0005(5) | 0.0066(4) |
| **Fe1** | 0.5 | 0.0 | 0.5 | 0.018(1) | 0.0074(7) | 0.0056(9) | 0.0061(9) | 0.0009(8) | 0.0011(5) | 0.0005(5) | 0.0066(4) |
| **Mg2** | 0.0075(3) | 0.1739(2) | 0.3084(2) | 0.95(1) | 0.0102(6) | 0.0036(7) | 0.0075(7) | 0.0032(6) | -0.0003(4) | 0.0002(4) | 0.0068(4) |
| **Fe2** | 0.0075(3) | 0.1739(2) | 0.3084(2) | 0.042(1) | 0.0102(6) | 0.0036(7) | 0.0075(7) | 0.0032(6) | -0.0003(4) | 0.0002(4) | 0.0068(4) |
| **Mg3** | 0.4878(2) | 0.8837(2) | 0.0771(2) | 0.9644(2) | 0.0084(6) | 0.0168(9) | 0.0075(8) | 0.0048(7) | -0.0003(4) | 0.0006(4) | 0.0107(5) |
| **Fe3** | 0.4878(1) | 0.8837(0) | 0.0771(0) | 0.035(2) | 0.0084(6) | 0.0168(9) | 0.0075(8) | 0.0048(7) | -0.0003(4) | 0.0006(4) | 0.0107(5) |
| **Si** | 0.0776(2( | 0.1403(1) | 0.7017(2) | 0.96(1) | 0.0056(4) | 0.0085(5) | 0.0054(5) | 0.0018(4) | -0.0001(3) | 0.0000(3) | 0.0066(3) |
| **O1** | 0.7757(5) | 0.0004(3) | 0.2959(4) | 1.0 | 0.0124(9) | 0.001(1) | 0.011(1) | 0.004(1) | 0.0004(8) | 0.0002(8) | 0.0080(5) |
| **O2** | 0.7274(5) | 0.2442(4) | 0.1284(4) | 1.0 | 0.0078(8) | 0.020(2) | 0.005(1) | 0.000(1) | -0.0000(7) | 0.0001(9) | 0.0118(6) |
| **O3** | 0.2249(5) | 0.1683(3) | 0.5281(4) | 1.0 | 0.0091(8) | 0.0099(1) | 0.006(1) | 0.001(1) | 0.0002(7) | -0.0002(8) | 0.0086(5) |
| **O4** | 0.2625(5) | 0.8576(4) | 0.2974(4) | 1.0 | 0.006(8) | 0.019(2) | 0.006(1) | 0.003(1) | 0.0001(7) | -0.0000(9) | 0.0109(6) |
| **O5** | 0.2637(7) | 0.0606(5) | 0.1057(5) | 1.0 | 0.018(1) | 0.028(2) | 0.019(2) | 0.010(2) | 0.011(1) | 0.005(1) | 0.0216(8) |
| **H** | 0.11(2) | 0.00(1) | 0.01(1) | 1.000(0) | 0.0544(0) | | | | | | |

There was slight ordering of $Fe^{2+}$ in chondrodite consistent with polyhedral volume. In chondrodite, the distortable M2 site had 4.2% $Fe^{2+}$ occupancy, the M1 site had 3.8% occupancy, and the smaller M3 site had 3.5% $Fe^{2+}$ occupancy. The single-crystal refinement confirmed the microprobe data, showing approximately 0.02 mol % $Fe^{2+}$ in the sample.

**Table 8.** Selected interatomic distances (Å) and geometrical parameters for synthetic chondrodite sample 407B. Notes: TAV = tetrahedral angle variance; TQE = tetrahedral quadratic elongation; OAV = octahedral angle variance; OQE = octahedral quadratic elongation.

| | | | | | |
|---|---|---|---|---|---|
| **Si-O1** | 1.6477(16) | **M2-O1** | 2.0202(17) | **M3-O1** | 2.2409(18) |
| **Si-O2** | 1.6464(17) | **M2-O2** | 2.2236(16) | **M3-O2** | 2.0150(18) |
| **Si-O3** | 1.6446(14) | **M2-O3** | 2.0413(15) | **M3-O2** | 2.1118(16) |
| **Si-O4** | 1.6124(15) | **M2-O3** | 2.1768(18) | **M3-O4** | 2.1379(15) |
| **<Si-O>** | 1.6377 | **M2-O3** | 2.1972(17) | **M3-O5** | 2.0592(19) |
| **Vol (Å$^3$)** | 2.2204 | **M2-O4** | 2.0644(20) | **M3-O5** | 2.0806(17) |
| **TQE** | 1.0103 | **<M2-O>** | 2.1289 | **<M3-O>** | 2.1076 |
| **TAV** | 46.1710 | **Vol (Å$^3$)** | 12.4726 | **Vol (Å$^3$)** | 12.1315 |
| | | **OQE** | 1.0221 | **OQE** | 1.0203 |
| **O5-O5** | 2.8281 | **OAV** | 74.5911 | **OAV** | 67.9199 |
| **O5-H** | 0.7709 | | | | |
| **O5-O1** | 3.0195 | | | | |

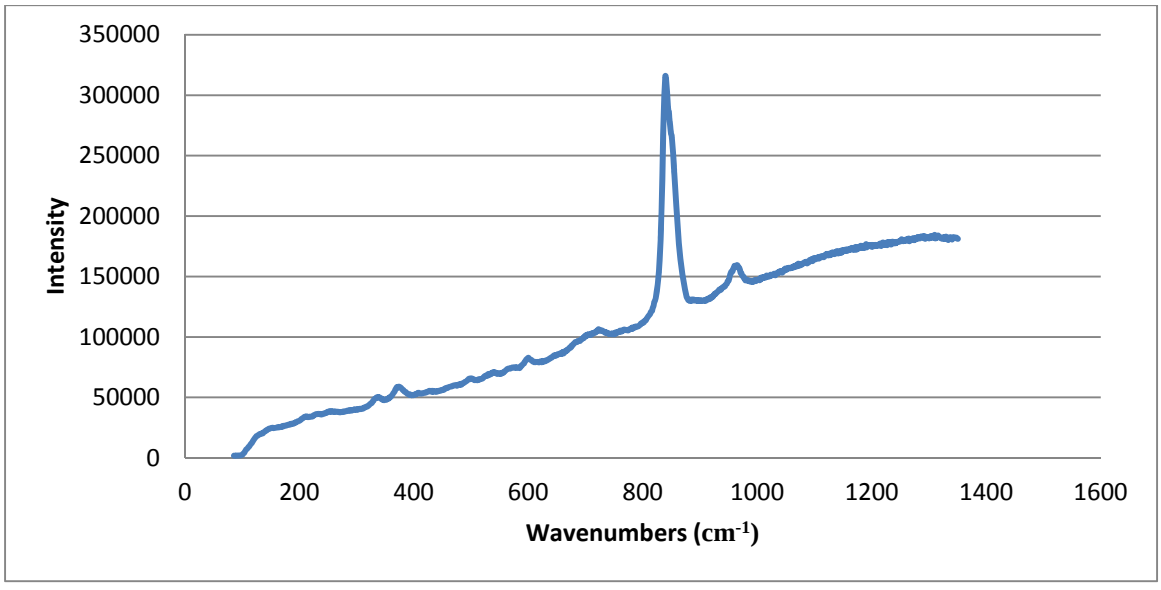


**Figure 13.** Raman spectrum of chondrodite corresponding to the normal vibrational modes at ambient temperature and pressure. Collected with a 532 nm wavelength laser line**.**

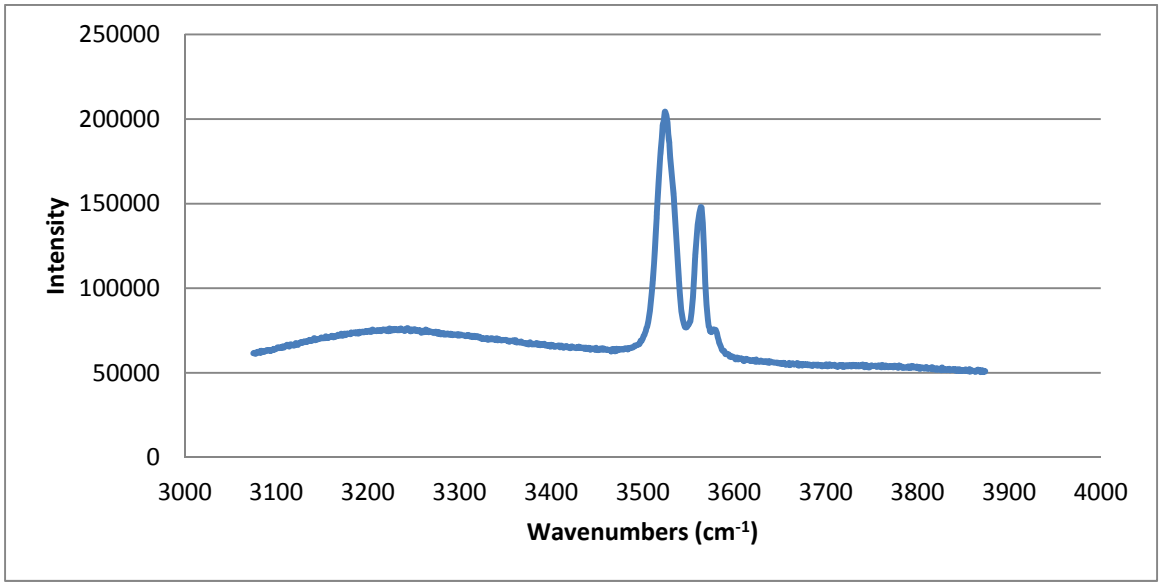


**Figure 14.** Raman spectrum of chondrodite corresponding to the OH-stretching modes at ambient temperature and pressure. Collected with a 532 nm wavelength laser line**.**

Chondrodite exhibits two strong peaks corresponding to the O-H stretching modes at 3527 $cm^{-1}$ and 3565 $cm^{-1}$ that have previously been observed by Lin et al. (1999) in another synthetic chondrodite sample. Lin et al. (1999) observed H-bonding peaks at 3226 $cm^{-1}$ and 2930 $cm^{-1}$. These peaks are much weaker than the strong doublet, and at least one peak was observed at 2966 $cm^{-1}$.

In order to examine the effects of protonation and $Ti^{4+}$ substitution in the humites, bond angle strains for a synthetic-chondrodite, a Ti-rich chondrodite, and a natural sample were compared in Table 9.

**Table 9.** Selected bond angles indicative of cation-cation repulsion in chondrodite samples of various chemical compositions. References: (1) Gibbs et al, 1970. (2) Fujino and Takeuchi, 1978, (3) this study.

| **Angle** | **0.35 OH/(OH+F)$_{(1)}$** | **0.58 OH/(OH+F)$_{(2)}$** | **1.00 OH/(OH+F)$_{(3)}$** |
|---|---|---|---|
| **O1-M1-O3** | -14.9 | -15.2 | -14.58 |
| **O2-M2-O3** | -18.3 | -19.6 | -18.5 |
| **O1-M3-O2** | -16.8 | -18 | -17.2 |
| **O4-M2-O2** | -7.0 | -11.5 | -10.5 |
| **O4-M3-O2** | -7.0 | -9.4 | -10.45 |

The O4-M2-O2 and O4-M3-O2 angle strains are the most drastic shifts in bond length. The strains in chondrodite also reflect the shift of the M3 cation in response to repulsion introduced by the H into the cavity. For both the synthesized OH-chondrodite and Ti-chondrite sample, there are significantly higher strains than those measured for the natural, low-$Fe^{2+}$ sample. For nearly all of the angles, the Ti-chondrodite shows higher strain than that of the OH-endmember. This could be explained by an additional strain introduced by $Ti^{4+}$ substitution.

**Clinohumite**

The unit cell parameters were refined to be a = 4.7524(4), b = 10.294(1), and 13.707(1) Å, α = 100.65(1)°, V = 659.04(4) Å$^3$.

**Table 10.** Atomic fractional coordinates and thermal displacement parameters for natural norbergite sample from Danbury, CT.

| Atom | *x/a* | *y/b* | *z/c* | occ* | $U_{11}$ | $U_{22}$ | $U_{33}$ | $U_{23}$ | $U_{13}$ | $U_{12}$ |
|---|---|---|---|---|---|---|---|---|---|---|
| **$Mg1_C$** | 0.5 | 0.0 | 0.5 | 0.748(3) | 1.21(4) | 0.0059(6) | 0.0033(6) | 0.0000(4) | 0.0008(3) | 0.0004(4) |
| **$Fe1_C$** | 0.5 | 0.0 | 0.5 | 0.251(3) | 0.0117(6) | 0.0059(6) | 0.0033(6) | 0.0000(4) | 0.0008(3) | 0.0004(4) |
| **$Mg1_N$** | 0.4977(2) | 0.9461(1) | 0.2741(1) | 0.979(7) | 0.0051(6) | 0.0059(6) | 0.0033(6) | 0.0000(4) | 0.0008(3) | 0.0004(4) |
| **$Fe1_N$** | 0.4977(2) | 0.9461(1) | 0.2741(1) | 0.021(7) | 0.0051(6) | 0.0059(6) | 0.0033(6) | 0.0000(4) | 0.0008(3) | 0.0004(4) |
| **Mg2** | 0.5102(2) | 0.2503(1) | 0.3881(1) | 0.453(6) | 0.0092(5) | 0.0084(5) | 0.0058(4) | 0.0000(0) | 0.0000(0) | -0.0007(3) |
| **Fe2** | 0.5102(2) | 0.2503(1) | 0.3881(1) | 0.046(6) | 0.0092(5) | 0.0084(5) | 0.0058(4) | 0.0000(0) | 0.0000(0) | -0.0007(3) |
| **$Mg2_S$** | 0.0095(2) | 0.1401(1) | 0.1699(1) | 0.979(7) | 0.0079(6) | 0.0076(7) | 0.0071(6) | 0.0031(4) | -0.0001(4) | 0.0001(4) |
| **$Fe2_S$** | 0.0095(2) | 0.1401(1) | 0.1699(1) | 0.020(7) | 0.0079(6) | 0.0076(7) | 0.0071(6) | 0.0031(4) | -0.0001(4) | 0.0001(4) |
| **Mg3** | 0.4925(3) | 0.8778(1) | 0.0430(1) | 1.000(8) | 0.0076(6) | 0.0101(7) | 0.0058(6) | 0.0010(4) | -0.0007(4) | 0.0005(4) |
| **Si1** | 0.0732(2) | 0.0661(1) | 0.3890(1) | 1.0 | 0.0058(4) | 0.0071(4) | 0.0055(4) | 0.0017(3) | 0.0001(3) | -0.0001(3) |
| **Si2** | 0.0762(2) | 0.1768(1) | 0.8354(1) | 1.0 | 0.0053(4) | 0.0077(5) | 0.0055(4) | 0.0021(3) | 0.0004(3) | -0.0000(3) |
| **O1,1** | 0.7333(5) | 0.0645(2) | 0.3879(2) | 1.0 | 0.0061(9) | 0.008(1) | 0.0053(9) | 0.0015(8) | 0.0001(7) | -0.0003(8) |
| **O1,2** | 0.2784(5) | 0.4199(2) | 0.3878(2) | 1.0 | 0.008(10) | 0.006(1) | 0.007(10) | 0.0017(8) | 0.0003(8) | 0.0012(8) |
| **O1,3** | 0.2222(5) | 0.1124(3) | 0.2932(2) | 1.0 | 0.008(10) | 0.009(1) | 0.0053(1) | 0.0033(8) | -0.0001(8) | -0.0007(8) |
| **O1,4** | 0.2221(5) | 0.1591(2) | 0.4859(2) | 1.0 | 0.007(10) | 0.009(1) | 0.0053(9) | -0.0001(8) | 0.0003(8) | 0.0001(8) |
| **O2,1** | 0.2364(5) | 0.3223(3) | 0.1623(2) | 1.0 | 0.005(10) | 0.010(1) | 0.007(10) | 0.0033(8) | 0.0002(8) | 0.0010(8) |
| **O2,2** | 0.7802(5) | 0.9685(2) | 0.1622(2) | 1.0 | 0.006(10) | 0.008(1) | 0.008(10) | 0.0029(8) | 0.0001(8) | -0.0002(8) |
| **O2,3** | 0.7238(5) | 0.2798(3) | 0.2622(2) | 1.0 | 0.006(10) | 0.009(1) | 0.008(10) | 0.0037(8) | 0.0003(8) | -0.0001(8) |
| **O2,4** | 0.7270(5) | 0.2270(3) | 0.0702(2) | 1.0 | 0.007(10) | 0.009(1) | 0.0061(9) | 0.0016(8) | 0.0006(8) | 0.0000(8) |
| **OH** | 0.2635(5) | 0.0464(2) | 0.0558(2) | 1.0 | 0.007(10) | 0.006(1) | 0.0065(9) | 0.0030(8) | 0.0029(8) | 0.0016(8) |
| **H1** | 0.1709(5) | 0.0174(3) | 0.0296(2) | 0.40000 | 0.05000 | | | | | |
| **H2** | 0.4467(5) | 0.0310(2) | 0.1302(2) | 0.40000 | 0.05000 | | | | | |

.

There was significant ordering of $Fe^{2+}$ in clinohumite. The M1 site exhibits 25.1% $Fe^{2+}$ occupancy and the $M2_6$ has 4.6% $Fe^{2+}$ occupancy.

**Table 11.** Selected interatomic distances (Å) and geometrical parameters for natural norbergite sample from Franklin, NJ.

| | | | | | |
|---|---|---|---|---|---|
| **Si1-O1,1** | 1.6108 | **$M2_5$-O1,3** | 2.0268 | **M3-O2,1** | 2.1214 |
| **Si1-O1,2** | 1.6532 | **$M2_5$-O2,1** | 2.1713 | **M3-O2,2** | 2.1906 |
| **Si1-O1,3** | 1.6315 | **$M2_5$-O2,2** | 2.0510 | **M3-O2,4** | 1.9994 |
| **Si1-O1,4** | 1.6350 | **$M2_5$-O2,3** | 2.1881 | **M3-O2,4** | 1.9994 |
| **<Si1-O>** | 1.6326 | **$M2_5$-O2,4** | 2.2112 | **M3-O5** | 2.0174 |
| **Vol (Å$^3$)** | 2.1974 | **$M2_5$-O5** | 2.0566 | **M3-O5** | 2.0372 |
| **TQE** | 1.0110 | **<$M2_5$-O>** | 2.1175 | **<M3-O>** | 2.0813 |
| **TAV** | 48.7982 | **Vol (Å$^3$)** | 12.2719 | **Vol (Å$^3$)** | 11.6701 |
| | | **OQE** | 1.0222 | **OQE** | 1.0181 |
| | | **OAV** | 74.4462 | **OAV** | 61.1945 |
| | | | | | |
| **Si2-O2,1** | 1.6109 | **$M2_6$-O1,1** | 2.1756 | **O5-O5** | 2.7754 |
| **Si2-O2,2** | 1.6419 | **$M2_6$-O1,2** | 2.0541 | **O5-O2,2** | 2.9582/3.0286 |
| **Si2-O2,3** | 1.6390 | **$M2_6$-O1,3** | 2.2014 | **O5-H1** | 0.6066 |
| **Si2-O2,4** | 1.6302 | **$M2_6$-O1,3** | 2.2014 | **O5-H2** | 1.3667 |
| **<Si2-O>** | 1.6305 | **$M2_6$-O2,3** | 2.0645 | | |
| **Vol (Å$^3$)** | 2.1917 | **$M2_6$-O2,3** | 2.0645 | | |
| **TQE** | 1.0100 | **<$M2_6$-O>** | 2.1302 | | |
| **TAV** | 44.5403 | **Vol (Å$^3$)** | 12.3994 | | |
| | | **OQE** | 1.0291 | | |
| | | **OAV** | 93.9072 | | |

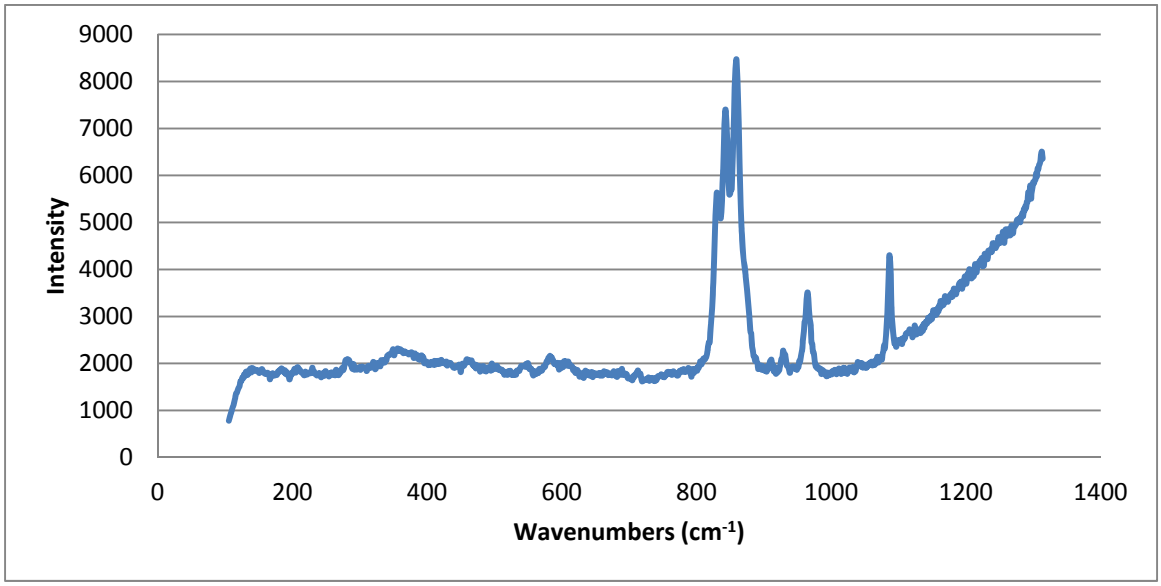


**Figure 15.** Raman spectrum of clinohumite corresponding to the normal vibrational modes at ambient temperature and pressure. Collected with a 785 nm wavelength laser line**.**

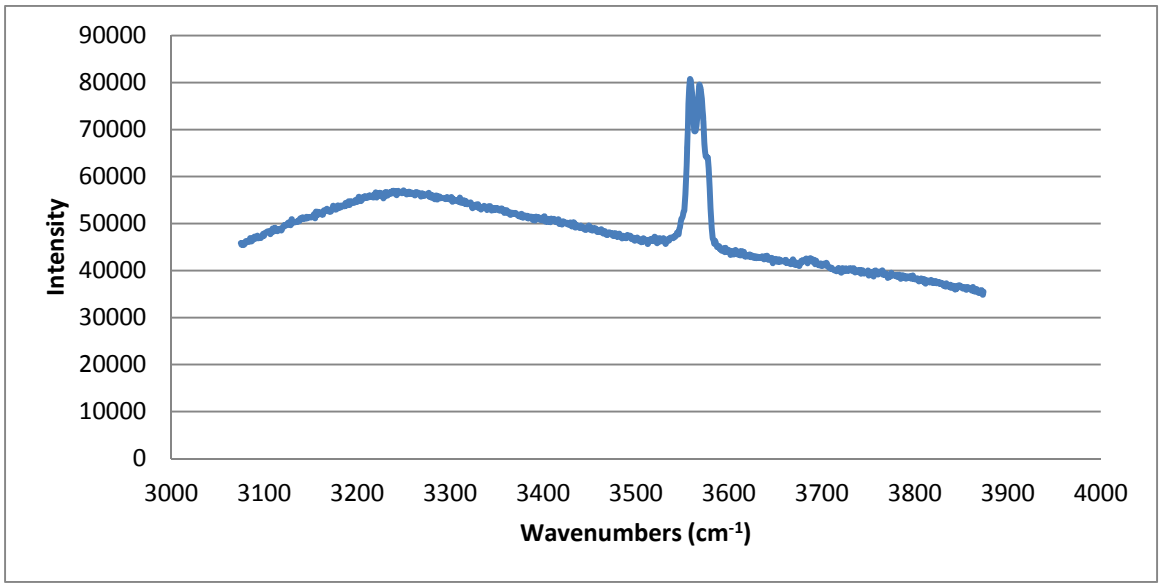


**Figure 16.** Raman spectrum of clinohumite corresponding to the OH-stretching modes at ambient temperature and pressure. Collected with a 532 nm wavelength laser line**.**

Clinohumite exhibits a strong doublet at 3569 cm-1 and 3570 cm-1.This matches the spectrum obtained by Frest et al. (2006) from a natural sample of clinohumite from Namibia.

**Norbergite**

The unit cell parameters were refined to be a = 4.692(4), b = 10.280(8), and 80762(4) Å, V = 422.60(50) $Å^3$.

**Table 12.** Atomic fractional coordinates and thermal displacement parameters for natural norbergite sample from Franklin, NJ.

| Atom | *x/a* | *y/b* | *z/c* | occ* | $U_{11}$ | $U_{22}$ | $U_{33}$ | $U_{23}$ | $U_{13}$ | $U_{12}$ | Atom |
|---|---|---|---|---|---|---|---|---|---|---|---|
| **Si** | 0.4195(1) | 0.7196(3) | 0.25 | 0.4833(1) | 0.0053(0) | 0.0088(5) | 0.0066(6) | 0.0000(5) | 0.0000(0) | -0.0000(0) | 0.0069(4) |
| **Mg3** | 0.989(2) | 0.6324(2) | 0.4308(1) | 0.9787(1) | 0.0081(0) | 0.0106(5) | 0.0067(6) | -0.0000(5) | 0.0004(4) | -0.0001(4) | 0.0085(4) |
| **Fe3** | 0.989(2) | 0.6324(2) | 0.4308(1) | 0.0032(1) | 0.0081(0) | 0.0106(5) | 0.0067(6) | -0.0000(5) | 0.0004(4) | -0.0001(4) | 0.0085(4) |
| **Ti3** | 0.989(2) | 0.6324(1) | 0.4308(1) | 0.025(4) | 0.0078(6) | 0.0102(6) | 0.0064(6) | -0.000(4) | 0.0004(3) | -0.0001(4) | 0.0082(4) |
| **Mg2** | 0.991(2) | 0.9070(3) | 0.2500(2) | 0.4719(0) | 0.0080(0) | 0.0095(7) | 0.0102(8) | 0.0000(7) | 0.0000(0) | 0.0010(0) | 0.0093(5) |
| **Fe2** | 0.991(2) | 0.9070(3) | 0.2500(2) | 0.0100(0) | 0.0080(0) | 0.0095(7) | 0.0102(8) | 0.0000(7) | 0.0000(0) | 0.0010(0) | 0.0093(5) |
| **O1** | 0.762(3) | 0.7217(6) | 0.25 | 0.5 | 0.0069(0) | 0.015(1) | 0.008(1) | 0.000(1) | 0.0000(0) | 0.0002(0) | 0.010(1) |
| **O2** | 0.277(3) | 0.5742(7) | 0.25 | 0.5 | 0.0108(0) | 0.011(1) | 0.009(2) | 0.000(1) | 0.0000(0) | 0.0011(0) | 0.010(1) |
| **O3** | 0.268(3) | 0.7915(4) | 0.1044(0) | 1.0 | 0.0097(0) | 0.012(1) | 0.009(1) | 0.000(1) | -0.0000(8) | -0.0008(8) | 0.0106(8) |
| **O5** | 0.729(3) | 0.9673(4) | 0.0831(0) | 1.0 | 0.0043(0) | 0.0030(8) | 0.0038(9) | -0.0000(8) | -0.0025(7) | 0.0008(6) | 0.0037(7) |

Norbergite had significant Ti occupancy, and Ti ordered into the M3 site according to size. Single-crystal refinements of norbergite confirmed the microprobe data, with 1.0 mol % Ti occupying the M3 site, and 0.3 mol % $Fe^{2+}$ occupying both the M3 and M2 sites.

**Table 13**. Selected interatomic distances (Å) and geometrical parameters for natural norbergite sample from Franklin, NJ.

| | | | | | |
|---|---|---|---|---|---|
| **Si-O1** | 1.6138(31) | **M2-O1** | 2.1896(22) | **M3-O1** | 2.1199(18) |
| **Si-O2** | 1.6371(14) | **M2-O2** | 2.0324(23) | **M3-O2** | 2.1664(22) |
| **Si-O3** | 1.6346(20) | **M2-O3 (x2)** | 2.1751(22) | **M3-O3** | 2.1193(17) |
| **Si-O3** | 1.6436(20) | **M2-O5 (x2)** | 2.0108(20) | **M3-O3** | 2.002(22) |
| **<Si-O>** | 1.6301 | **<M2-O>** | 2.0990 | **M3-O5** | 1.9891(14) |
| **Vol (Å$^3$)** | 2.1901 | **Vol (Å$^3$)** | 11.9505 | **M3-O5** | 2.0239(19) |
| **TQE** | 1.0100 | **OQE** | 1.0226 | **<M3-O>** | 2.0698 |
| **TAV** | 43.9980 | **OAV** | 73.3785 | **Vol (Å$^3$)** | 11.5356 |
| | | | | **OQE** | 1.0176 |
| **O5-O5** | 26.888 | | | **OAV** | 57.7487 |
| **O5-O1** | 2.9189 | | | | |

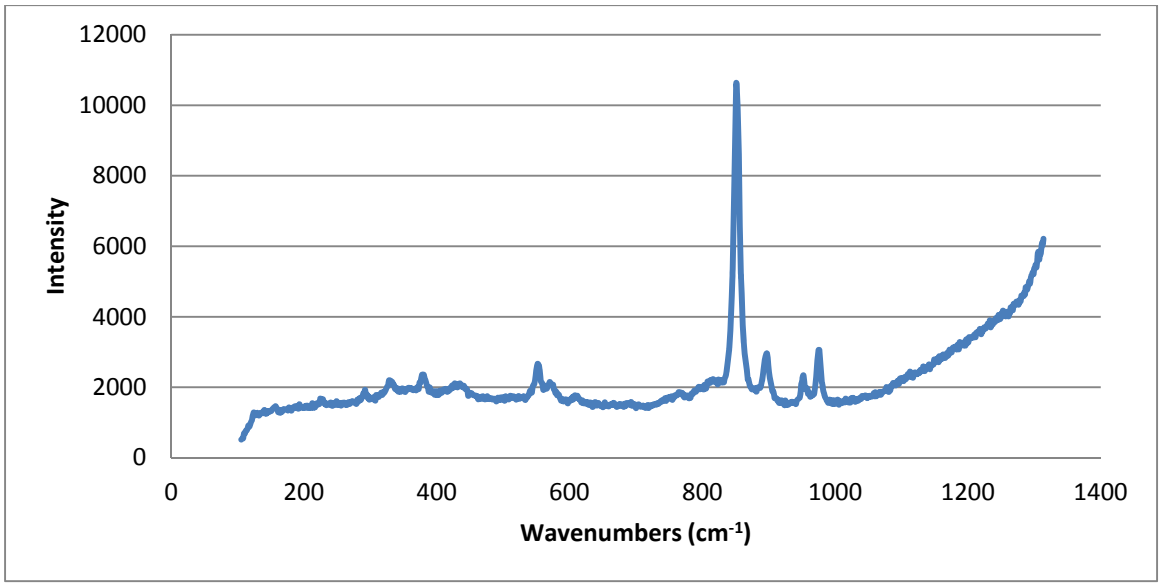


**Figure 17.** Raman spectrum of norbergite corresponding to the normal vibrational modes at ambient temperature and pressure. Collected with a 785 nm wavelength laser line**.**

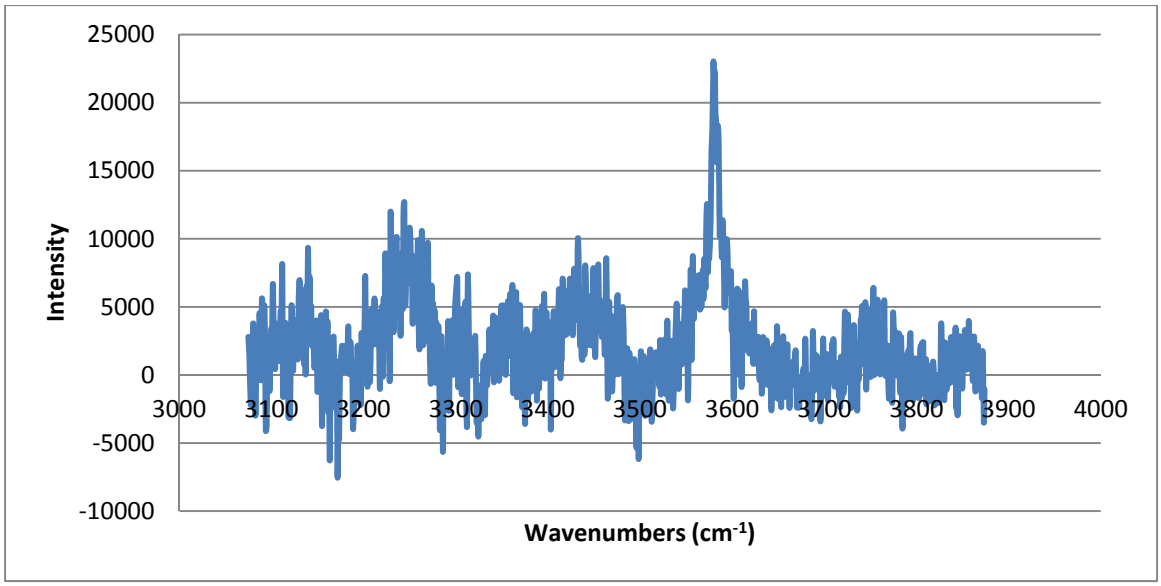


**Figure 18.** Raman spectrum of norbergite corresponding to the O-H stretching modes at ambient temperature and pressure. Collected with a 532 nm wavelength laser line**. Please put the cm-1 numbers at bottom.**

One very weak band was observed in the natural norbergite sample at 3580 cm-1, and a similar peak was observed by Liu et al. (1999) at 3573 cm-1 in a sample also from Franklin, New Jersey. It has been observed that not all stretching bands can be observed in a single grain (Liu et al., 1999), and this study only measured the spectra on one grain.

**Effects of $Ti^{4+}$ substitution and protonation on structure**

It has been observed that cation repulsion introduced by the proton increases the M3-O5 bond length in OH-rich humites (Friedrich et al., 2001). $Ti^{4+}$ substitution also affects the $M2_5$ polyhedron. Ti orders to the M3 site, and therefore the bonds in this site (particularly M3-O2,2) are strengthened (Friedrich et al., 2001). Consequentially, the $M2_5$-O2,2 bond length in increased. The $M2_5$-O2,2 bond length is also increased because it participates in hydrogen bonding. Table 14 compares data from this stud to data in the literature to provide insight on the effects of protonation and $TI^{4+}$ substitution on different bond lengths.

**Table 14.** Bond lengths indicative of hydrogen incorporation. References: (1) Friedrich et al., 2001 (2) This study (3) Friedrich et al., 2002 (4) Gibbs and Ribbe, 1969 (5) Ribbe and Gibbs, 1971.

| | **OH/(OH+F)** | **Ti content (wt % TiO)** | **M3-O5** | **$M2_5$-$O_6$(mean)/$M2_4$** | **$M2_5$-O2,2/O1, $M2_4$-O3** |
|---|---|---|---|---|---|
| **Chondrodite** | $0.42_{(1)}$ | 0.16 | 2.055(9) | 2.13 | 2.07(1) |
| | $1.00_{(2)}$ | 0.00 | 2.0806(17) | 2.129 | 2.0702(17) |
| **Clinohumite** | $0.61_{(2)}$ | 0.08 | 2.0372(2) | 2.1175 | 2.0510 |
| | $1.00_{(3)}$ | 5.40 | 2.05(2) | 2.134 | 2.080 |
| **Norbergite** | $0.09_{4)}$ | 0.42 | 1.986 | 2.104 | 2.188 |
| | $0.39_{(2)}$ | 0.99 | 2.02324(23) | 2.0990 | 2.1751(22) |
| **Humite** | $0.47_{(5)}$ | 0.10 | 2.032(4) | 2.122 | 2.065(4) |
| | $0.67_{(7)}$ | 0.26 | 2.0392 | 2.0993 | 2.0544 |

It is evident that protonation is the primary control of expansion of M3-O5 bond. All humite minerals exhibit significant increase of the M3-O5 bond with increasing OH content. However, the M25-O2,2/O1, M24-O3 bond does not follow such a rigid pattern. This bond is affected significantly by both $Ti^{4+}$ substitution and protonation. For example, in the Ti-rich and OH-rich chondrodite samples, the $M2_5$-O1 bond is nearly the same. Both titanium and hydrogen effectively lengthen the bond in the Ti-rich sample, making it as long as the OH-chondrodite.

Norbergite does not have an $M2_5$ site. Rather, it has a $M2_4$ site, and the oxygen that would H-bond is O3. An increase in the $M2_4$-O bond with increasing H and Ti-content is(?) not observed in this bond, as would be expected. It is possible that norbergite does not experience strong H-bonding. The presence of the two monovalent anions in the $M2_4$ site can displace the M cation 0.1 Å from the center of the polyhedron (Camara,1997). Because of this displacement, the charge density of the oxygen atom would be most strong directed toward the center of the polyhedron, and extending this distribution in

the opposite direction would be unfavorable. Neutron diffraction work would be a helpful next step in elucidating the role that H-bonding plays in stabilizing different types of humite minerals.

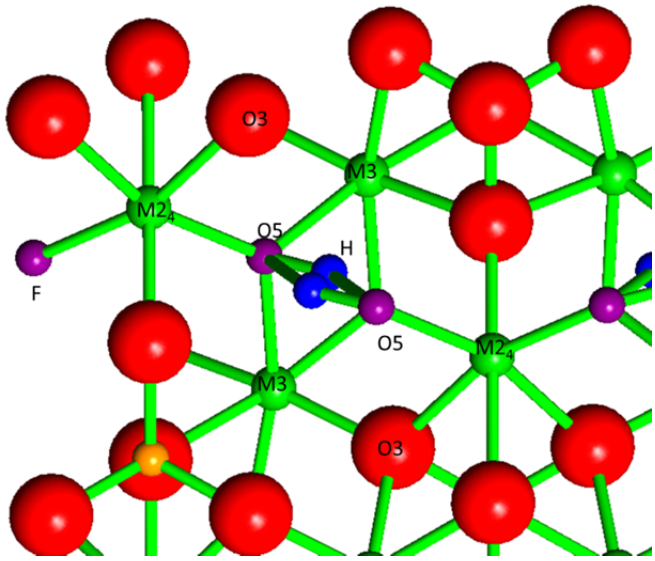


**Figure 19.** Environment surrounding H-incorporation in norbergite.

It is unclear why the orthorhombic OH-humite end-members seem to be rarer than OH-clinohumite and OH-chondrodite. Studies from Abbott et al (1989) have shown that potential energy wells of equivalent energies corresponding to the H1 and H2 positions are found in equivalent chemical locations in all the humite minerals. Hydrogen bonding is known to play a key role in the stabilization of hydrated structures. If hydrogen bonding is minimized in norbergite because of the increased number of monovalent anions per formula unit, this could mean OH-norbergite would be relatively unstable in comparison to the other humite minerals.

Since both of the M3-O5 and M25-O2,2/O1 bonds lie almost parallel to the b-axis, this leads to expansion of the b-axis. Because this is the least rigid axis in the structure, it is the primary controlling factor in the cell volume. Ribbe (1979) derived a linear relationship between the size of the monovalent anion and the cell volume. This suggests that as protonation increases, the cell volume increases linearly, as shown in Figure 20.

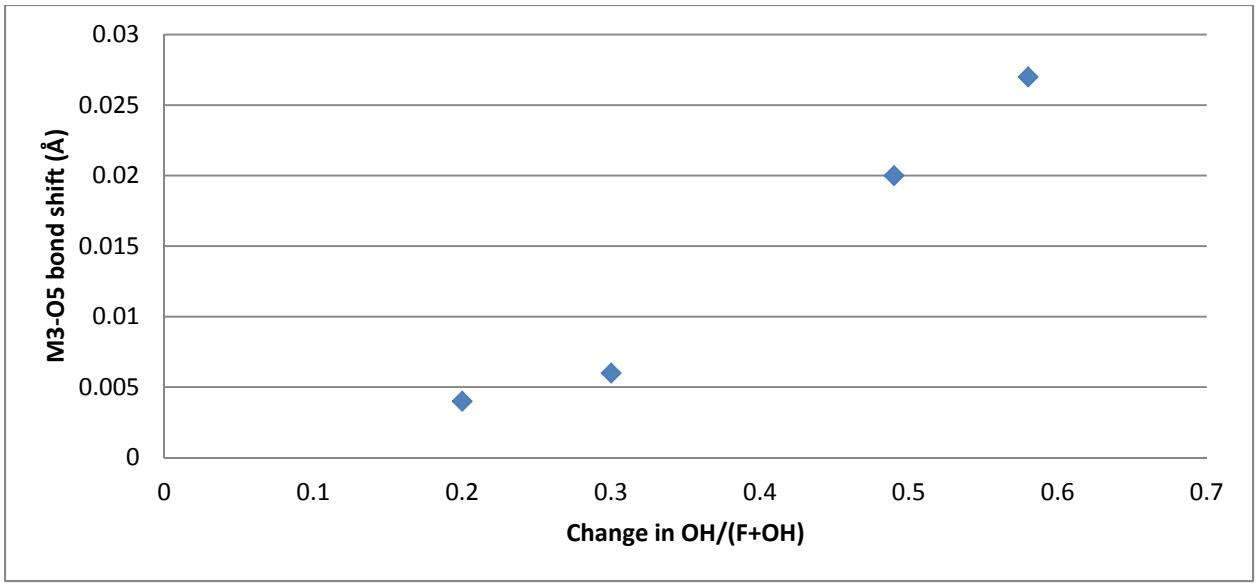


**Figure 20.** Bond length differences vs degree of protonation difference for humite minerals.

The monoclinic humite minerals are able to incorporate hydrogen accompanied by large bond length shifts relative to the bond shifts associated with protonation of orthorhombic humites. One may infer that monoclinic humites are able to accommodate these drastic bond shifts whereas orthorhombic humites are not.

**Effects of anion repulsion**

Anion repulsion also plays a significant role in structure determination of the humites, particularly with regard to hydrogen incorporation. Since the site in which hydrogen is incorporated in a site of major significance in determining the cell volume and compressibility, anion repulsion has major effects on overall cell properties as well. Examination of Table 15 reveals that O5-O5 distances are greater in monoclinic cells than orthorhombic. Because these distances are greater, there is more room for incorporation of polar molecules into the monovalent anion site**.**

**Table 15.** Average O5-O5 bond distances for humite minerals of various chemical compositions. References: (1) Gibbs et al., 1970 (2) This study (3) Friedrich,2001 (4) Gibbs and Ribbe, 1969 (5) Ribbe and Gibbs, 1971.

| Mineral | OH/(OH+F) | O5-O5 bond distance (Å) | <M3-O> avg distance |
|---|---|---|---|
| **Chondrodite** | $0.35_{(1)}$ | 2.972 | 2.078 |
| | $1.00_{(2)}$ | 2.8281 | 2.1076 |
| **Clinohumite** | $0.61_{(2)}$ | 2.7754 | 2.0813 |
| | $1.00_{(3)}$ | 2.958 | 2.088 |
| **Norbergite** | $0.10_{(4)}$ | 2.689 | 2.068 |
| | $0.39_{(2)}$ | 2.689 | 2.0698 |
| **Humite** | $0.47_{(5)}$ | 2.786 | 2.086 |
| | $0.67_{(2)}$ | 2.772 | 2.0786 |

When one considers the strain induced by protonation, these data suggest the orthorhombic cell is already tightly constrained and does not have the ability to fully incorporate hydrogen without destabilizing the structure. More compressibility data on a wider range of chemical compositions of humite minerals would be a logical next step to exploring this hypothesis.

In conclusion, this study has presented the first successful refinement of hydrogen in the humite structure and has identified two distinct H positions in the humite structure. H1 has been identified as the dominant site via X-ray diffraction.

The introduction of $Ti^{4+}$ and $H^{+}$ into the humite structures increases bond angle strains associated with cation shifts, particularly in the M2 polyhedra. Further evidence was presented for the stabilizing effects of H-bonding and the role of anion repulsion in determination of humite structures.

**REFERENCES**

Abbott, R.N., Jr., Burnham, C.W., Post, J.E.(1989) Hydrogen in humite-group minerals: Structure-energy calculations. American Mineralogist, 74, 1300-1306.

Akaogi, M. Akimoti, S. (1980) High-pressure stability of a dense hydrous magnesian silicate $Mg_{23}Si_8O_{42}H_6$ and some geophysical implications. Journal of Geophysical Research, 85. 6944-6948.

Aoki, K., Fujino, L. and Akaogi, M. (1976) Titanochondrodite and titanoclinohumite derived from the upper mantle in the Buell Park kimberlite. Arizona, U.S.A. Contributions to Mineralogy and Petrology, 56, 243-253.

Bell, D.R., and Rossman, G.R. (1992) Water in earth's mantle: The role of nominally anhydrous minerals. Science, 255, 1391-1397.

Berry, A.J., and James, M. (2002) Refinement of hydrogen position in natural chondrodite by powder neutron diffraction: implications for the stability of humite minerals. Mineralogical Magazine, 66, 441-449.

Berry, A.J., and James, M. (2001) Refinement of hydrogen positions in synthetic hydoxyl-clinohumite by powder neutron diffraction. American Mineralogist, 86, 181 – 184.

Bolfan-Casanova, N., Keppler, H., Rubie, D.C. (2000) Water partitioning between nominally anhydrous minerals in the MgO-$SiO_2$-$H_2O$ systems of up to 24 GPa: implications for the distribution of water in the Earth's mantle. Earth and Planetary Science Letters, 182, 209-221.

Burnley, P.C., and Navrotsky, A. (1996) Synthesis of high=pressure hydrous magnesium silicates: Observations and analysis. American Mineralogist, 81, 317 – 326.

Camara, F. (1997) New data on the structure of norbergite: location of hydrogen by x-ray diffraction. The Canadian Mineralogist, 35, 1523-1530.

Downs, R.T., Zha C., Duffy, T.S., Finger, L.W. (1996) The equation of state of forsterite to 17.2 GPa and effects of pressure media. American Mineralogist, 81, 51 – 55.

Farrugia, L.J. (1999) WinGX software package. Journal of Applied Crystallography, 32, 837-838.

Friedrich, A., Lager, G.A., Kunz, M., Chakoumakos, B.C., Smyth, J.R., Schultz, A.J. (2001) Structure-dependent single-crystal neutron diffraction study of natural chondrodite and clinohumites. American Mineralogist, 86, 981-989.

Friedrich A., Lager G.A., Ulmer, P., Kunz, M., Marshall, W.G. (2002) High-pressure single-crystal X-ray and powder neutron study of F,OH/OD-chondrodite: Compressibility, structure, and hydrogen bonding. American Mineralogist, 87, 931-939.

Fujino, K., Takeuchi, Y. (1978) Crystal chemistry of titanian chondrodite and titanian clinohumite of high-pressure origin. American Mineralogist, 63, 535-543.

Galsukin, E.V., Gazeev, V.M., Lazic, B., Armbruster, T., Galuskina, I.O., Zadov, A.E., Pertsev, N.N., Wrzalik, R., Dzierzanowski, P., Gurbanov, A.G., and Bazowska, G. (2009) Chegemite $Ca_7(SiO_4)_3(OH)_2$ – a new humite-group calcium mineral from the Northern Caucasus, Kabardino-Balkaria, Russia. European Journal of Mineralogy, 21, 1045-1059.

Gibbs G.V., and Ribbe, P.H. (1969) The crystal structures of the humite minerals: I. Norbergite. American Mineralogist, 54, 376-390.

Gibbs, G.V., and Ribbe, P.H., Anderson, C.P. (1970) The crystal structures of the humite minerals. II. Chondrodite. American Mineralogist, 55, 1182-1194

Lager, G.A., Ulmer P., Miletich, R., Marshall W.G. (2001) O-D···O bond geometry in OD-chondrodite. American Mineralogist, 86, 176-180.

Langer, K., Platonov, A.N., Matsyuk, S.S., Wildner, M. (2002) The crystal chemistry of the humite minerals: $Fe^{2+}$-$Ti^{4+}$ charge transfer and structural allocation of $Ti^{4+}$ in chondrodite and clinohumite. European Journal of Mineralogy, 14, 1027-1032.

Lin, C.-C., Liu, L.-G., and Mernagh, T.P., and Irifune, T. (2000) Raman spectroscopic study of hydroxyl-clinohumite at various pressures and temperatures. Physics and Chemistry of Minerals, 27, 320-331.

Lin, C.-C., Liu L.-G., and Irifune, T. (1999) High-pressure Raman spectroscopic study of chondrodite. Physics and Chemistry of Minerals, 26, 226-245.

Liu, L., Lin, C., Mernagh, T.P. (1999) Raman spectra of norbergite at various pressures and temperatures, American Mineralogist, 11. 1011-1021.

McGetchin, T.R., Silver, L.T., and Chodos, A.A. (1970) Titanoclinohumite: A possible mineralogical site for water in the upper mantle. Journal of Geophysical Research, 75, 255-259.

Satish-Kumar, M., and Niimi, N. (1998) Flourine-rich clinohumite from Ambasamudram marbles, Southern India: mineralogical and preliminary FTIR spectroscopic characterization. Mineralogical Magazine, 62, 509-519.

Ottolini, L., Fernando, C., Bigi, S. (2000) An investigation of matrix effects in the analysis of fluorine in humite-group minerals by EMPA, SIMS, and SREF. American Mineralogist, 85, 89-102.

Prasad, P.S.R., and Sarma, L.P. (2004) A near-infrared spectroscopic study of hydroxyl in natural chondrodite. American Mineralogist, 89, 1056-1060.

Ribbe, P.H. (1979) Titanium, fluorine, and hydroxyl in the humite minerals. American Mineralogist, 64, 1027-1035.

Ribbe, P.H., and Gibbs, G.V. (1971) Crystal structures in the humite minerals: III. Mg/Fe ordering in humite and its relation to other ferromagnesian silicates. American Mineralogist, 56, 1155-1173.

Ross, N.L., and Crichton, W.A. (2001) Compression of synthetic hydroxlyclinohumite [$Mg_9Si_4O_{16}(OH)_1$] and hydroxlychondrodite [$Mg_5Si_1O_8(OH)_2$]. American Mineralogist, 86, 990-996.

Robinson, K, Gibbs, G.V., Ribbe, P.H. (1973) The Crystal Structure of the Humite Minerals. IV. Clinohumite and Titanoclinohumite. American Mineralogist, 58, 43-49.

Sheldrick, G.M. (1997) SHELXL97, Release 97-2. Program for the refinement of crystal structures. University of Göttingen, Germany.

Smyth, J.R. (2006) Hydrogen in high pressure silicate and oxide mineral structures. Reviews in Mineralogy and Geochemistry, 62, 85-116.

White, T.J., Hyde, B.G. (1982) Electron microscope study of the humite minerals: I. Mg-rich specimens. Physicla Chemistry of Minerals, 8, 55-63.

Williams, Q. (1992) A vibrational spectroscopic study f hydrogen in high pressure mineral assemblages. In Y. Syono, M.H Manghnani, Eds., High-Pressure Research: Application to Earth and Planetary Sciences, Geophysical Monograph Series, 67, 289-296.

Wirth, R., Dobrzhinetskaya,L.F., Green II, H.W. (2001) Electron microscope study of the reaction olivine + $H_2O$ + $TiO_2$ → titanian clinohumite + titanian chondrodite synthesized at 8 GPa, 1300 K. American Mineralogist, 86, 601-610.

Wunder, B., Mendenbach, O., Daniels, P., Schreyer, W. (1995) First synthesis of the hydroxyl end-member of humite, $Mg_7Si_2O_{12}(OH)_2$. American Mineralogist, 80, 638-640.

Yamamoto, K., and Akimoto, S. (1974) High-pressure and high-remperature investigations in the system MgO-$SiO_2$-$H_1O$. Journal of Solid State Chemistry, 9, 187-195.

Yamamoto, K., and Akimoto, S (1977). The system MgO-$SiO_2$-$H_1O$ at high pressures and temperatures – stability field for hydroxyl-chondrodite, hydroxyl-clinohumite and 10 Å-phase. American Journal of Science, 277, 288-312.